ADDIS ABABA UNIVERSITY

ADDIS ABABA INSTITUTE OF TECHNOLOGY

SCHOOL OF GRADUATE STUDIES

CONSTRUCTION QUALITY MONITORING OF EMBANKMENT DAMS USING PORE WATER PRESSURE THE CASE OF KESEM DAM

A Thesis Submitted to the School of Graduate Studies of Addis Ababa University in Partial Fulfillment for the Requirements of the Degree of Master of Science in Civil and Environmental Engineering (Major in Hydraulic Engineering)

BY

ABEBE AREGA TADESSE

ADVISOR

Dr. Ing. MEBRUK MOHAMMED

November, 2014

ADDIS ABABA UNIVERSITY
ADDIS ABABA INSTITUTE OF TECHNOLOGY
SCHOOL OF GRADUATE STUDIES

CONSTRUCTION QUALITY MONITORING OF EMBANKMENT DAMS USING PORE WATER PRESSURE, THE CASE OF KESEM DAM

A Thesis Submitted to the School of Graduate Studies of Addis Ababa University in Partial Fulfillment for the Requirements of the Degree of Master of Science in Civil and Environmental Engineering (Major in Hydraulic Engineering)

BY

ABEBE AREGA TADESSE

APPROVED BY BOARD OF EXAMINERS:

Bikila Teklu (Dr.) ----------------------- -------------
Chairman (department of graduate committee) Signature Date

Mebruk Mohammed(Dr.Ing) ----------------------- ------------
Advisor Signature Date

Daneal F/Sellassie (Dr.)
----------------------- ---------------
Internal Examiner Signature Date

Ase Kemal (Dr.) ----------------------- -----------------------
External Examiner Signature Date

CERTIFICATION

The undersigned, certify that I have read the thesis entitled "Construction Quality Monitoring of Embankment Dams using Pore water pressure, The Case of kesem Dam" and here by recommended for acceptance by the Addis Ababa University in partial fulfillment for the requirement of the degree of Master of Science in Civil and Environmental Engineering major in Hydraulic Engineering.

____

Dr. Ing. Mebruk Mohammed

(Advisor)

____

Date

DECLARATION AND COPYRIGHT

I, the undersigned, declare that this thesis is my own original work and it has not been presented and will not be presented by me to any other University for the similar or any other degree award.

Declared by:

Name: ________________________________

Signature: ____________________________

Date: _________________________________

ACKNOWLEDGEMENTS

I would first and foremost like to thank my advisor Dr.-Ing. Mebruk Mohammed for giving me the opportunity to do this thesis under his supervision, for his invaluable advice and continuous supports of all kind throughout the research period. My thanks extend to my friends Fekremariam Negash and Bahru Mekuria. This dissertation is a result of the research work that was carried out mainly at the Department of Civil and Environmental Engineering, Addis Ababa University Institute of Technology, where I have benefited a lot from the inspiring and friendly atmosphere. Thanks are due to all members of the department.

Data used for the case study of this research were obtained from Water Works Design and Supervision Enterprise, Water Works Construction Enterprise and Kesem Dam site, Ethiopia.

My parents have always a special place in my life. I cannot thank you enough Alem Kebede and Arega Tadesse for being good and loving parents to me. If I possess any good qualities, it is all because of you. My brothers and sister, I owe you a big thank you for your supports and love all along.

Above all, it is due to the ALMIGHTY GOD for all his blessings; through him all things is possible .In him, I put my trust for protection and guidance.

Abebe Arega.

October, 2014.

TABLE OF CONTENTS

LIST OF FIGURES

LIST OF TABLES

LIST OF ABBREVIATIONS AND SYMBOLS

D	Dispersive
ND	Non Dispersive
WL(RWL)	Reservoir Water level
el	elevation
a.s.l	above sea level
USACE	United States Army Corps of Engineers
ANN	Artificial Neural Network
FEM	Finite Element Method
V	Velocity
K	Hydraulic conductivity (permeability)
i	Hydraulic gradient
OMC	Optimum Moisture Content
MDD	Maximum Dry Density
AS	Australian Standard
μ	dynamic fluid viscosity
d_m	mean grain size
WWDSE	Water Works Design and Supervision Enterprise
WWCE	Water Works Construction Enterprise
L.L	Liquid Limit
P.L	Plastic Limit
P.I	Plastic Index
ADAS	Automatic Data Acquisition Systems
OGL	Original Ground Level
k	intrinsic Permeability
H	pressure head

etc.	et cetera
SCADA	Supervisory Control And Data Acquisition
2-D	2 dimensional
3-D	3 dimensional
e.g	for example
lab.	Laboratory
MPL	Measured Pore Pressure
R^2	Coefficient of determination
AAU	Addis Ababa University
AAiT	Addis Ababa Institute of Technology

ABSTRACT

Monitoring pore water pressure within earth and rock fill dams has been practiced extensively with safety probably being the first and the most important reason for it. The overall objective of the research is to propose construction quality monitoring technique in embankment dams using pore water pressure by taking Kesem dam.

For Kesem dam, the construction quality monitoring was done by making sure that an arbitrary core sample tested in a laboratory has brought about the expected hydraulic conductivity. Such approach seldom represents the whole core safety for the expected hydraulic conductivity. This research has used the pore pressures measured in the sensors located inside the core of the dam. Seepage flow inside an embankment dam can be predicted using SEEP/W software. However, this model needs accurate hydraulic conductivity value, which is very difficult/costly to obtain. As long as dam monitoring is concerned accurate prediction of pore pressures is required. To make sure that such needed accuracy is obtained a two phase modeling is proposed in this study. At first, SEEP/W will predict a pore pressure at sensor locations for different values of hydraulic conductivity. These predicted values together with the reservoir water level are then used as an input to a Multiple Linear Regression (MLR) model. The coefficients of multiple linear regression models are estimated by making use of previously measured pore pressure values at the sensors.

The coefficients obtained have resulted in an R^2 value of nearly unity. This indicates the result of the pore water pressure in the piezometric areas from the model is almost the same as the result obtained from the recorded data. Hence, it can be concluded that the technique of construction quality monitoring used in Kesem dam has promising application if used.

Key words

Embankment Dam Construction Monitoring, Kesem Dam, Pore water pressure, SEEP/W, Reservoir water level, Hydraulic conductivity, Pore pressure sensor, MLR

1. INTRODUCTION

1.1. General

Dams are barrier structures built to block the flow of water. Because of changes of geology and other criteria of dams; these structures may also change. For these reasons, dams should certainly be designed and built with high assurance for a long duration of time. Awareness of such changes is related to the government, dam owners and the specified surrounding community. Special devices are required to predict dam's behavior. Water through reservoir may possibly move behind the dams and under the foundations. Seepage flow of water through porous media depends on the soil media, type of flow, properties of liquid and hydraulic gradient. Water running from dam's reservoir, especially from earth dams has important role on dam stability [11]. Water leakage on earth dams and its method of seepage control is the first step of designing embankment dams. Science and technologies related to basic seepage rules have given necessary information to scientists to control and overcome any encountered problems. Recently, many scientists studied and analyzed the effective parameters on seepage process and they were able to solve many cases by designing issues. However, each dam has its own configuration and descriptive design. Special attention is required to know detail information about the seepage, dam foundation, borrowing materials and type of design.

The two principal types of embankment dams are earth and rock-fill dams, depending on the predominant fill materials used. An earth fill dam is constructed primarily of engineering soils compacted uniformly and intensively in relatively thin layers and at controlled moisture contents. Thus, earth fill dams, constituent over 50% selected soil material. On the other hand, rock fill embankment dams are constructed of rock fill materials which contain over 50% compacted rock fill materials [19]. The second types of dams are concrete dams which are constructed of mass concrete. Concrete dams are classified in two three main categories. These are gravity, arch and buttress dams.

Kesem dam is a rock fill embankment dam with a crest width and length of respectively 10m and 720m. A good rock fill dam is one of the safest structures if a very careful attention is given to its construction for the following factors [17]:

- Strength and volume change characteristics of the rock fill materials under high confining pressures with particular attention to the time effect on strength, pore pressures, consolidation and strains;
- Flow net of seepage through and /or under the dam;
- Sliding factors for rock fill on foundation contact surfaces;
- Cracking with in embankments;
- Control of compaction to minimize irregularity of settlement between zones;
- Slope correction of abutments, under core and filters;

In this research, SEEP/W model has been applied to predict pore water pressure and seepage line. The desired methods of control and monitoring techniques of measuring the pore water pressure using installed instrument recorded data and some physical and geometrical characteristics of dams have been applied and extensively investigated.

1.2. Statement of the Problem

Dams are one of the most important civil engineering structures not only because of they are constructed with heavy cost but also due to their importance in multidisciplinary economic and social values.

Ethiopia is undertaking a number of dams for different purposes. Proper monitoring of construction quality in dams particularly embankment dams is vital for the future safety operation and economical optimization.

Monitoring of construction quality in this dam is vital to know and study characteristics of other dams to be built in the future and to assess existing conditions of previously constructed dams.

Since Kesem dam is constructed on hot volcanic areas, studying the construction quality monitoring activities which are mainly related to pore water pressure has tremendous advantages.

Thus, good construction quality method adopted will minimize the amount of water seeping through the dam and foundation and increase safety of the dam.

The parameters such as hydraulic conductivity and pore water pressure have to be controlled and monitored based on the design and laboratory results. There should be a means to regulate the construction quality for safe and economical construction of embankment dams. Besides these, the construction quality checkup systems are required for safety and ease of construction especially in high embankment dams such as Kesem dam. As high pore water pressure is induced on the impervious zone of embankment dams , the use of this pore water pressure as an important parameter is vital not only for Kesem dam but also to draw a valid conclusion for other embankment dams since they have an impervious zone for checking up of seepage.

Construction quality monitoring in embankment dams mainly concerned with pore water pressure and seepage has significant role in monitoring activities during and after construction of dams. Quality monitoring activities of embankment dams using pore water pressure was not a common methodology in the past and this is one of the problem statements but in the future it will be one of economical method for monitoring safety of dams during construction.

1.3. Objective of the Research

General Objective: - the overall objective of the research is to design construction quality monitoring techniques in embankment dams using pore water pressure

Specific Objectives

- Proposing a method of monitoring safety of embankment dam
- Monitoring effects of hydraulic conductivity variation on pore pressure development
- Assessing existing dam safety monitoring techniques

1.4. Organization of the Thesis

Apart from the introduction in chapter one, the fundamental theories and principles of construction monitoring of dams are laid in chapter two. Towards the end of this chapter extensive review is given.

Chapter three deals with the methodology used, over view of the recorded data, simulation methods including the identification of important data for analysis of Kesem dam and piezometric locations and selection of critical points.

Chapter four focuses on the results and discussion of the simulated and monitored values and parameters. Finally, in chapter five conclusions and some suggestions for future research are presented.

The thesis has appendices giving some basic analysis results. In the main body of the thesis references to the different sections of the appendix will be made as appropriate.

2. LITERATURE REVIEW

Construction monitoring in different civil engineering disciplines is vital for safe and economical operation of projects. Construction monitoring for dams, ground water investigation and tunnel operation, for bearing capacity investigation of soils etc.is required. Various parameters are used as controlling mechanisms for different construction projects. Use of pore pressure as means of monitoring the effect of shaft excavation, as well as to manage the works of excavation, grouting, lining of shaft wall and related excavation works in Mizunami Underground Research Laboratory (MIU) construction site in central Japan was used [8]. The researchers used Finite Element Method (FEM) and Artificial Neural Network (ANN) and reach with a very good agreement on the performance of the model they used.

Monitoring of seepage quantity and quality once the filter is functioning is very important to the safety of the embankment dam. An increase in seepage flow may be due to a higher reservoir level or may be cause by cracking or piping. The source of the additional seepage should be determined and action taken as required. Decreases in seepage flows may also signify dangers such as clogging of the drain(s) with piped material, iron oxide, calcareous material, effects of remedial grouting, etc. Again, the cause should be determined and appropriate remedial measures should be taken. Drain outlets should be kept free of sediment and vegetation. In cold climates, design or maintenance measures should be taken to prevent clogging of drain outlets by ice [2].

2.1 Kesem Dam

The main components of Kesem dam project are to build a dam to retain the Kesem River flow occurred during the rainy season, divert the river flow into the downstream canalization and irrigate the land of 20,000 ha in the Kesem, Kebena and Bolahamo. The reservoir of the project is shown in Fig.2.1 below.

Figure 2.1 Kesem Dam Reservoir

It is a rock fill dam with a central clayey core. The dam has a maximum construction height of 96 m. The crest is 720 m long and 10 m wide with an elevation of 941.00m from the mean sea level. Upstream dam slope in an order of 1:2.25 and downstream slope of 1:2.0. The core has a slope of 1:0.25 with a minimum width of 4m [9].

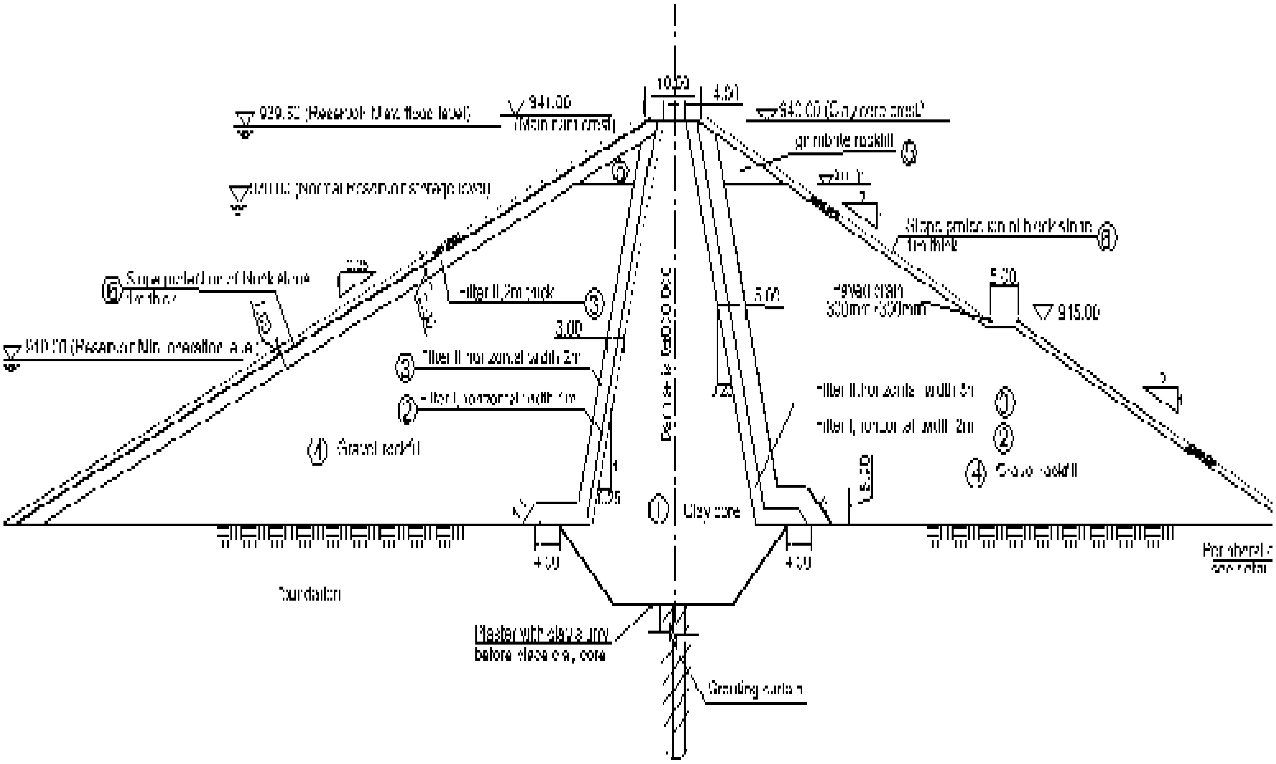

Figure 2.2 Kesem Dam Section 3-3

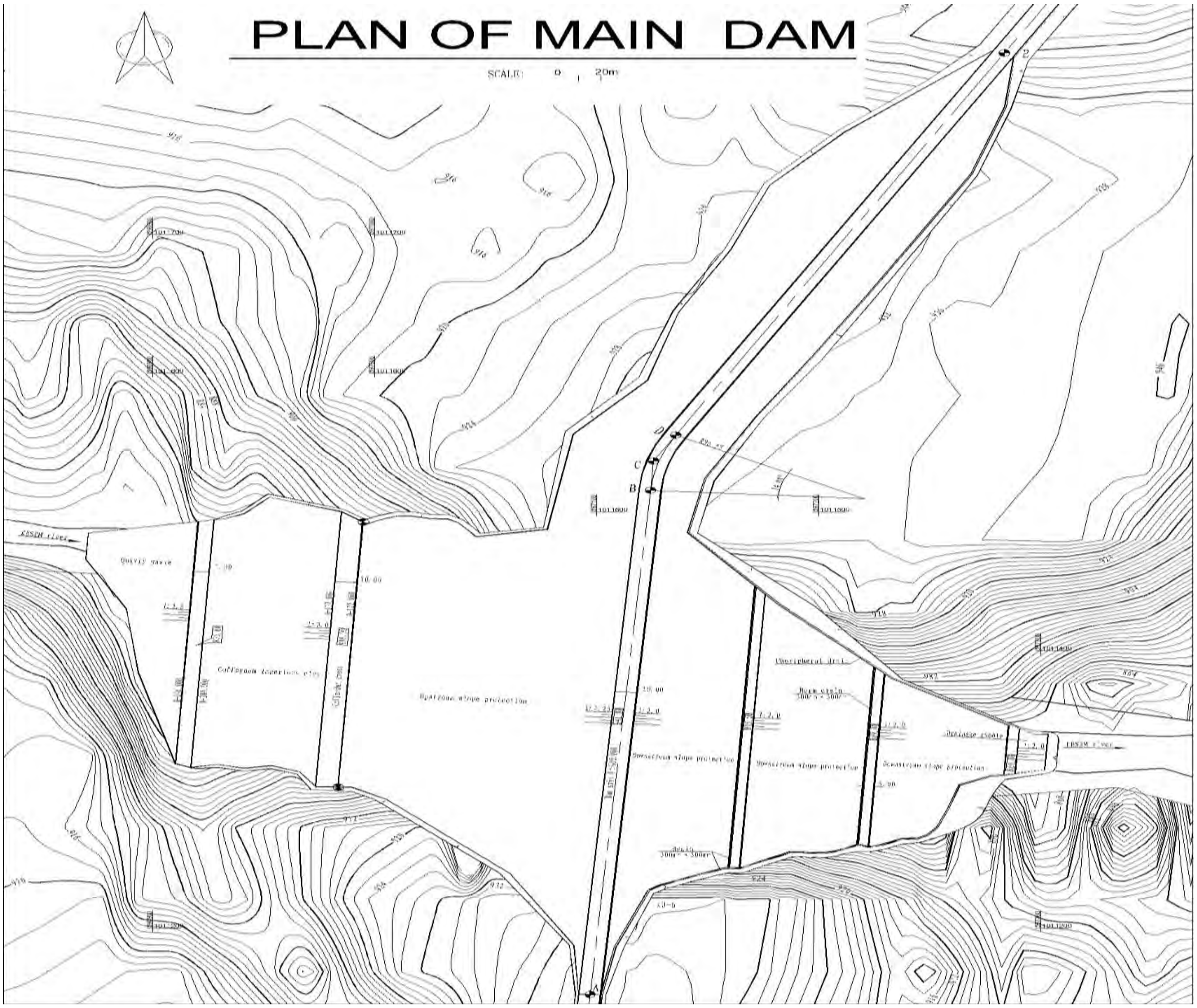

Figure 2.3 Plan of Kesem Dam Axis

Various types of instruments such as electromagnetic settlement gage, inclinometer, displacement sensors, pore water pressure in dam, dam foundation pore water pressure, contact earth pressure cell, water level probe etc. were installed throughout the dam at different elevations. These instruments were installed at four monitoring sections. Thirty piezometers were mounted at these sections. The highest monitoring section of the dam is section 3-3. Heads monitored by piezometers at section 3-3 at different elevations were investigated in this study.

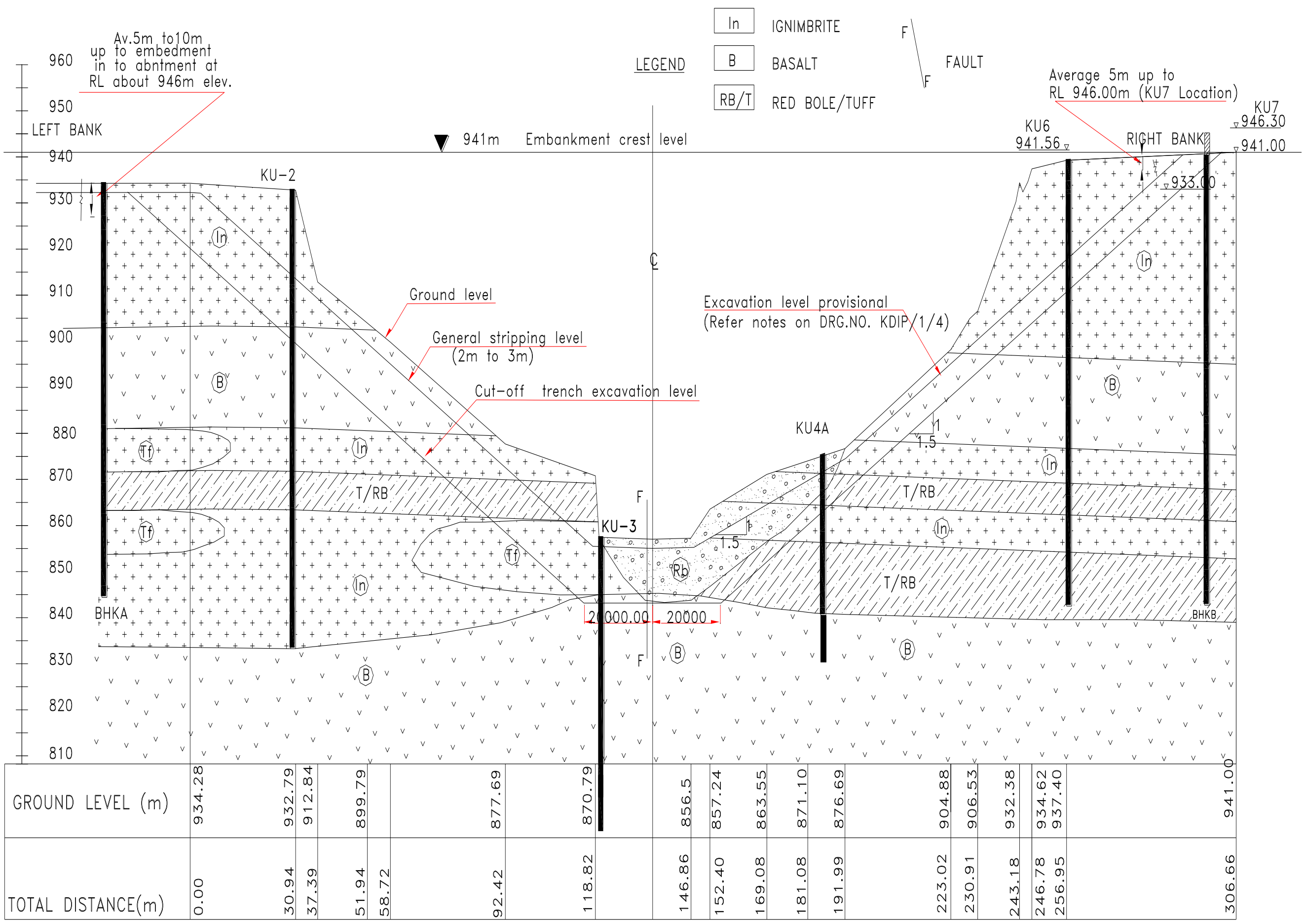

Figure 2.4 Longitudinal Profile Along Kesem Dam Axis

Figure 2.5 Photo of Dam Cross Section Down Stream View

2.2 General Construction Considerations

Weather and ground-water conditions during construction may significantly alter water contents of proposed fill material, or create seepage and/or hydraulic conditions, necessitating modifications in design. Projects must be continuously evaluated and re-engineered, as required, during construction, to ensure that the final design is compatible with conditions encounter during construction. Design and design review personnel will make construction site visits to determine whether design modifications are required to meet actual field conditions. Site specific conditions must be given attention in construction operations. For example, when high embankments are constructed in narrow valleys, it may be possible to place fill rapidly, which will increase pore-pressure build up in the embankment and/or foundation [2]. Rather than reduce the rate of fill place unduly, it may be desirable to use flatter slopes, add stabilizing berms, or build the embankment in stages.

While test data and instrument observations provide more detailed and quantitative information than visual observations, they serve principally to strengthen and supplement visual observations of the embankment and foundation as the various construction activities are going on. Field forces should be constantly on the alert for conditions not anticipated in the design, such as excessively soft areas in the foundation; jointing, faulting, and fracturing in rock foundations; unusual seepage; bulging and slumping of embankment slopes; excavation movements; cracks in slopes; and the like.

It is particularly important to make observations during the first filling of the reservoir as weaknesses in a completed dam often show up at this time. Visual observations of possible distress such as cracking, the appearance of turbid water in downstream toe drainage systems, erosion of riprap, soft wet spots downstream of the abutments or at the downstream toe or on the downstream slope, and other observations are important. Observations of instrumentation also yield valuable data in this respect.

2.2.1 Compaction

Compaction is the process of densifying soil and reducing air voids by applying mechanical energy. Compaction increases the strength, lowers the compressibility and reduces the permeability of a soil by rearranging its constituent materials.

Compaction should be undertaken by using a tamper foot roller, commonly referred to as a sheep foot roller.

For all dams greater than 3meters the following activities should be done to obtain the required compaction [1]:

- All fill material for the embankment should be placed in layers (or lifts) no greater than 150mm thick.
- The largest size particle should not be greater than 1/3rd
  the height of the lift, that is, 50mm
- Each layer should be thoroughly compacted before the next layer is placed. A minimum of 6 passes to achieve the required compaction effort is generally required by a suitable machine (see below).
- The compaction effort achieved should be on average 98% Standard Maximum Dry Density (MDD) (non-structural fill) as in context to Modified MDD (structural fill) as per Australian Standard: AS1289.0-2000 Methods of testing soils for engineering purposes.
- The minimum compaction effort should be 95% Standard MDD. If the range of compaction effort varies throughout the dam, then it can lead to the dam embankment for differential settlement causing the embankment of the dam to crack. This may ultimately lead to leakage and dam failure.

The material forming the embankment should be placed with sufficient moisture to ensure proper compaction. If the material is too dry, water should be added. If the material is too wet it should be spread and mixed. Before each additional 150mm lift is added to the embankment, the preceding lift should be scarified to ensure that the two lifts are properly joined so that no natural paths for seepage are present that may result in dam failure. A wheeled scraper or truck should be used for placing the clay on the dam site. The clay should then be spread by the use of the blade on a tamper foot roller or from a bulldozer towing a tamper foot roller (sheepsfoot roller).

Vehicles with crawler tracks are not suitable, as high compaction levels are not achieved. Likewise, compaction using a scraper tyre should not be used as the required compaction effort will not be achieved.

2.3 Construction Monitoring

Monitoring pore water pressure within earth and rock fill dams has been practiced extensively with safety probably being the first and the most important reason for it. Piezometers are the most common devices utilized for this purpose. Readings of a piezometer may also be used for monitoring the seepage, examining the effectiveness of the drains and cutoffs, and analyzing pore water pressure in dams during construction, impoundment, and rapid draw downs.

2.3.1 International Experiences of Construction Monitoring

In 1971, construction of an earth dam commenced in Mozambique where the right bank of the dam had a uniform 3-km-long cross section. Following the first impoundment, problems such as the formation of lagoons, saturated spots, and very high differences between predicted and measured amounts of seeping water and pore water pressures in the foundation of the dam were noted [10].

Pore water pressure in the 15-Khordad dam in Iran, an earth fill dam constructed in a V-shaped valley, with a clayey core and a height of 96 m was investigated following its construction. Many vibrating-wire and standpipe piezometers were installed in the body of the dam. Pore water pressure monitoring was made from one week to ten months following the impoundment. The core was modeled by a finite element mesh, transient and steady state analyses of pore pressures were performed and the results were compared with the monitored data. The trend in the monitored pore pressure was well modeled by the transient analysis. The researchers concluded that pore pressures in the cores of embankment dams may not achieve steady state conditions in some months, following the dam construction and impoundment. It was also observed that the selection of conductivity as a function of suction did not affect the results of modeling [4].

Monitoring of embankment dams, besides the visual inspection (qualitative data) and collection of environmental data (rainfall, seismic activity, and meteorological conditions), is usually grouped into geotechnical and geodetic surveying methods. Geotechnical monitoring may be divided into physical and deformation (geometric) measurements. The physical measurements include pore pressure measurements in critical areas of the dam and in its foundation; measurements of seepage through the dam and abutments; and measurements of stresses, using, e.g., earth pressure cells, within the selected locations in the dam. The deformation measurements typically involve settlement measurements, structural tilt monitoring and foundation displacements and deformations using e.g., extensometers and inclinometers. Geodetic monitoring determines vertical and horizontal absolute displacements of selected points at the crest and on the surface faces of the dam with respect to reference points located in a stable area using terrestrial and satellite positioning techniques. With the recent technological advancement in terrestrial surveying methods, robotic total stations with the automatic target recognition are commonly used to provide 3-D positioning information at preselected time intervals with the telemetric data acquisition. Here are some of the international experiences adopted in construction monitoring of different dams [15].

a. Instrumentation

The purpose of instrumentation and monitoring is to maintain and improve dam safety by providing information to 1) evaluate whether a dam is performing as expected and 2) warn of changes that could endanger the safety of a dam.

Pore pressures and uplift pressures are typically the least certain loads on a dam. Wherever reasonable, estimates of the pressures used in stability analyses should be verified by measurements. Redundant piezometers should be considered. Pore pressures should be measured in all existing observation wells and piezometers within an embankment and within the foundation. Installation of pore pressure instrumentation at existing dams is not required unless they do not meet stability criteria using a conservative estimate of the phreatic surface or anomalous conditions are suspected [6].

Existing dams that do not meet stability criteria using a conservative estimate of the phreatic surface should have instruments to locate the phreatic surface. If existing instrumentation is not adequate to do so, additional instruments should be installed. Instrumentation should be located based on the site-specific geotechnical characteristics of the embankment, foundation, and abutments. Typically, a minimum of two or three piezometers along a transverse line through the maximum section are sufficient. Piezometers are one of the most common devices utilized for monitoring pore water pressure in earth dams. Their readings reflect how different elements of a dam such as core, and embankment operate. Various types of piezometers are installed in an embankment dam; standpipe and vibrating wire being the most famous ones. Usually, piezometers diversity makes it possible to compensate their drawbacks [5].

Monitored pore water pressure heads during 15 month of first and second impoundments were investigated on Molasadra dam, Iran. Three dimensional seepage flows were modeled by finite element method at both transient and steady sate according to appropriate initial and boundary conditions. Seep3D software, provided by GEOSLOPE International Ltd, was used to perform the analysis. Modeled pore water pressure heads were compared to monitored heads, and the response of heads in core due to construction and impoundments were discussed. In addition, the effects of change in certain input parameters, such as conductivity as a function of pore water pressure, on the results were investigated [4].

b. Temperature Measurements

Temperature measurements can be used to provide valuable information about seepage flow and ongoing internal erosion in embankment dams. In Sweden the method has been frequently employed [14].

The first example involves a dam where a visual leakage was observed. Temperature measurements using conventional temperature sensors in standpipes were included together with standard methods in an extended monitoring program before, during and after the repair of the dam. The measured parameters seepage, pressure and temperature were evaluated jointly and provided a strong interpretation of the resulting performance of the dam repair.

The second example is from a dam where long term temperature measurements indicate a sudden seepage increase followed by a return almost to levels before the increase. Thereafter the temperature indicates roughly constant flow rates. The event may be interpreted as ongoing internal erosion followed by self repair. The final example treats automatic seepage evaluation from continuous distributed temperature sensing in optical fibers. Optical fibers have been installed in about 50 Swedish dams making such measurements viable. Some of these dams are equipped with an instrument permanently stationed for continuous measurements, and recently a novel automatic seepage evaluation routine has been taken into operation. The dam was constructed without drainage system, and has no possibilities to measure the seepage flow in a conventional way. It is several kilometers long and the entire length can be covered by the cable offering possibilities to both measure the seepage flow, and to detect sudden leakage changes. Selected data is exported to the dam owners Supervisory Control And Data Acquisition (SCADA) system. The system provides valuable information about seepage flow and improves the possibilities to discover decreasing dam performance [23].

The method uses the natural seasonal temperature variation that occurs in all surface water (such as lakes, reservoirs and rivers). The seepage flow causes a seasonal temperature variation inside the dam. This seasonal temperature variation inside the dam can be measured and used to evaluate the seepage flow. Generally, a constant temperature will indicate a small seepage, while large seasonal variations may indicate significant seepage. Larger seasonal temperature variations and shorter time lag between the temperature in the water and inside the dam indicate higher seepage. Increasing seepage causes increased annual temperature variation, and shorter time lag between the temperature in the water and inside the dam.

c. Geodetic Monitoring Surveys

Deformation monitoring of large dams and their surroundings supplies information on the behavior of the structure and its interaction with the bedrock. Monitoring results may also be used in verifying design parameters where the geotechnical parameters are of the highest importance. The determination of geotechnical parameters may be done in situ or in the laboratory. In laboratory testing, the selected samples may differ from one location to another, they may be disturbed during the collection, or the laboratory loading conditions may differ from natural conditions. Therefore, the comparison of the monitored data with the predicted data obtained during the design may give important information concerning the quality of the accepted geotechnical parameters [15].

In the United States earth fill dam projects consisting of Geodetic monitoring survey includes [20]:

- West Dam, about 87 m high and 2.7 km long,
- East Dam, 56 m high and 3.2 km long, and
- Saddle Dam, 39 m high and 0.8 km long

Fully Distributed Sensing

A method for seepage and settlement monitoring in earth embankment dams using fully distributed sensing along optical fibers is proposed. The database in the control and maintenance center is described. The configuration of optical sensing cable in series of embankment dams is developed. The simulated seepage flows under various flow rates are monitored using the optical fibers. A partial settlement within the embankment dam model is observed. The continuously decreasing temperature curve shows an abrupt dramatic increasing rate, which shows that the change is not caused by the temperature of the seepage water but the strain.

The three critical components of a dam monitoring system are 1) instrumentation, 2) data collection, and 3) data processing and management. Currently, there are many tools available for making improvements in these three areas and optimizing a dam's monitoring system [16].

d. Recent Developments in Geotechnical Instrumentation for Dam

Geotechnical instrumentation covers a range of sensors and instruments to monitor static parameters such as pore water pressure in soils and rock, settlement, horizontal displacements and earth pressure in embankments, strain and loads in anchors and reinforcing elements, tilt and inclination in slopes and retaining walls, as well as several other critical parameters for the long term stability of structures built with or on geological materials.

For a number of years exceeding half a century, most geotechnical instruments have been based on the vibrating wire measuring principle, except for tilt and inclination measurements where a number of measuring principles have been used, including servo---accelerometers, electrolytic tilt sensors and more recently MEMS (micro---electro mechanical systems) accelerometers.

ADAS (Automatic Data Acquisition Systems) are an important part of a dam monitoring program. Because of the specificity of the conditions of their deployment in outdoor, spread-out and sometimes harsh conditions, ADAS used for those applications need to have a number of features and functionalities which are discussed in the presentation, including low power consumption, modularity, network configurations options, network access options and real-time monitoring.

The advent of low-power low-cost radios that open the possibility of eliminating all surface cable runs on dams is also discussed.

2.3.2 Construction Monitoring Ethiopian Experiences

For Ethiopian context, there are devices which will be installed to measure a particular parameter of interest for monitoring of dam construction besides the laboratory tests and visual inspections. These parameters include stress inside the dam, seepage flows, seepage water clarity, piezometric levels, water levels, deformations or movements, pressures, loading conditions, temperature variations, or the accelerations experienced by the dam during an earthquake. The measurement from the instrument may be electronic or made by using a mechanical device.

Instrumentation is typically provided at dams to deal with informational needs that are most efficiently and effectively addressed by installing and reading instruments. Instrumentation is used in conjunction with other available information gathering approaches to comprise the complete monitoring program for a dam. Piezometers are one of the most common devices utilized for monitoring pore water pressure in most of Ethiopian dams.
The procedures followed in Kesem dam construction were as follows:

A production test is the first step in the dam construction before dam filling activity. After the test, the test report is submitted to the supervision engineer and to the design unit. They used this report after approval or further clarification as a base for the dam construction quality control standard [12]. Compaction is one of the major controlling factors during embankment dam construction.

Table 2.1 Summary of Clay Test Results (Lab. Result from Kesem Dam Optim. Report 2008)

Parameter	CB-2,TP-2 (0.0-2.0m)	CB-2,TP-6 (0.0-1.10m)	CB-2,TP-6 (1.10-2.50m)	CB-2,TP-8 (0.0-0.90m)	CB-2,TP-8 (0.90-2.70m)	CB-2,TP-12 (0.0-1.30m)	CB-2,TP-12 (1.30-2.40m)	CB-2,TP-12 (2.40-3.00m)	CB-2,TP-13 (1.10-2.00m)
Specific gravity	2.67	2.61	2.60	2.64	2.70	2.66	2.51	2.62	2.66
Grain size analysis									
Clay %	28.00	18.30	6.00	23.50	0.00	35.00	18.00	2.00	11.00
Silt %	42.01	59.52	65.67	48.95	65.10	45.85	59.97	50.49	50.65
Sand %	29.99	22.18	28.33	27.55	34.90	19.15	22.03	47.51	38.35
Gravel %	-								
Atterberg limits									
L.L %	61.75	42.07	38.70	48.49	31.79	54.30	46.18	32.80	39.35
P.L %	27.22	26.53	N.PL	29.49	N.PL	31.28	27.28	N.PL	21.42
P.I %	34.53	15.54	-	19.00	-	23.02	18.90	-	17.93
MDD(g/cm^3)	1.572	1.528	1.368	1.601	1.423	1.430	1.537	1.419	1.694
OMC (%)	24.90	24.60	28.40	23.50	30.20	29.80	24.80	26.80	19.40
Free Swell (%)	65.00	47.50	15.00	50.00	10.00	65.00	50.00	10.00	32.50
Shrinkage limit %	16.46	7.50	1.71	11.75	1.43	12.00	8.07	2.04	6.07
Dispersion	N.D	D	N.D	N.D	D	D	N.D	D	N.D

2.3.3 Advantages and Disadvantages of the Methods

Improper construction monitoring of dams can be a potential cause of financial loss. The dam constructed in any site can be used for irrigation, water supply, hydropower or any other purposes. So, if there is no proper monitoring during construction, it means losing of one or all of the above mentioned advantages of dams.

Regarding Geodetic monitoring and geotechnical measurements, both of them are equally important for the safe operation of the dam if proper usage is included.

Thus, geotechnical measurements and geodetic surveys complement each other in providing internal and surface information on the dam stability. Certainly, both types of instrumentation, if properly calibrated and installed, can serve as a warning system in case of an abnormal behavior of the dam. But the errors for the instruments during data collection may lead wrong decision.

In fully distributed sensing the information from the monitoring center provides important reference for the expert decision-making system to ensure the safety of the embankment dam long running. But the errors on the three critical components of a dam monitoring system that are on instrumentation, data collection, and data processing and management may lead to wrong decision and cause economic loss.

2.4 Seepage Analysis

Seepage analysis plays an important role in embankment dam engineering. It is required in different scenarios such as in volume change prediction, ground water contamination control, monitoring of leakage amount, slope stability analysis and design of earth structures.

The flow net solution for simple unconfined flow cases without boundary conditions for linear partial differential equation has three basic assumptions [18]:

- the soil is isotropic
- homogenous
- water flows only in saturated zone

The seepage problems which are studied in geotechnical engineering are mostly assumed to be laminar flow as they obey Darcy's law.

$$V = K\, i \qquad (2.1)$$

Seepage in embankment dams occurs through the foundation, embankment body or through both parts. Although applying a correct set of boundary conditions is vital in obtaining reliable results from seepage analyses in heterogeneous embankment dams, such boundary conditions are usually applied using certain simplifications. Simplifications of boundary conditions are applied in different ways at the upstream shell, the core, the filters, and the downstream shell. A simple, but a common approach in the finite element or finite difference seepage analysis is to eliminate the shells and the filters because of their high permeabilities. In this approach, only the core is modeled and the reservoir elevations along with the known downstream pore pressures are applied as the upstream and downstream boundary conditions, respectively [4].

2.5 Pore Water Pressure

Pore water pressure can be defined as pressure experienced by water contained in the pores of earth materials, concrete structures or rock. Via instrumentation associated with large civil engineering structures such as dams, underground tunnels, tall buildings and other mega structures measurement of pore water pressure enables to study detail geotechnical aspects of the structures.

The study of pore pressure has following main purposes:

- Effect of water in pores of soil or rock is to reduce load bearing capacity of soil or rock. Effect is more pronounced with higher pore water pressure leading eventually in some cases to total failure of load bearing capacity of the soil.
- Ground water level and flow pattern determination
- Determine flow pattern of water in embankment & concrete dams and their foundations and to delineate the phreatic line.

2.5.1 Model for Estimating Pore water Pressure at the End of Construction

Excess pore water pressure is developed in highly compressive, low permeability soils. But this pore water pressure dissipated through time and this might have adverse effect on the stability of the structures such as dams during and immediately after construction. So it is important to know the magnitude of pore water pressure developed at a certain level during construction. Based on the value determined a possible solution will be recommend for the safety of construction and to alleviate problems. For example, it might be recommended to have a stage construction to allow sufficient time to observe settlement.

Various researchers conducted a test on pore water pressure developed in embankment dams. The methods proposed for estimating pore pressure differs based on given conditions such as the type of model and target of modeling.

According to Hilf, the pore water pressure built up during construction is given by

$$\Delta u = \frac{p_o \delta}{(V_a + H_e V_w) - \delta} \qquad (2.2)$$

Where Δu the increase of pore water pressure due to increase in total stress applied under undrained conditions

V_a and V_w are ,respectively, air and water content in unit of volume soil, δ is amount of volume compression, and H_e and p_o are Henry's coefficient of solubility(usually $H_e = 0.02$) and the atmospheric pressure.

2.5.2 SEEP/W Model

SEEP/W is a finite element CAD software product for analyzing groundwater seepage and excess pore-water pressure dissipation problems within porous materials such as soil and rock. Its comprehensive formulation enables to consider analyses ranging from simple, saturated steady-state problems to sophisticated, saturated / unsaturated time-dependent problems. SEEP/W can be applied to the analysis and design of geotechnical, civil, hydrogeological, and mining engineering projects [23].

It is a numerical model that can mathematically simulate the real physical process of water flowing through a particulate medium. This model is purely mathematical and in this sense is very different than scaled physical modeling in the laboratory or full-scaled field modeling. It is important to understand that numerical modeling products like SEEP/W will have limitations that are related to the current capability of hardware or integral to the formulation of the software, since it was developed to consider specific conditions. SEEP/W is formulated only for flow that follows Darcy's law. Near the ground surface moisture may leave the ground as vapor. This component is not included in the SEEP/W formulation, like it is in another product of Geo-studio called VADOSE/W. SEEP/W can model both saturated and unsaturated flow, a feature that greatly broadens the range of problems that can be analyzed. In addition to traditional steady-state saturated flow analysis, the saturated / unsaturated formulation of SEEP/W makes it possible to analyze seepage as a function of time and to consider such processes as the infiltration of precipitation.

SEEP/W has limitations when it comes to modeling moisture leaving the system at the ground surface. A real physical model would not have this type of limitations.

This important point to remember is that the mathematical formulations implemented in software like SEEP/W result in a very powerful and versatile means of simulating real physical processes.

It can sometimes be different to obtain the appropriate input parameters or functions that are required for seepage analysis. SEEP/W has various function estimate techniques built into the software and also has a library file, included in the examples folder, which contains soil property functions for 24 different soils.

There are two fundamental types of finite element seepage analysis, steady-state and transient. Numerous additional constraints and conditions can be applied within each fundamental type [13]. After solving seepage analysis, SEEP/W offers many tools for viewing results. Generate contours or x-y plots of any computed parameter, such as head, pressure, gradient, velocity, and conductivity. Velocity vectors show flow direction and rate. Transient conditions can be shown as a changing water table over time. Interactively query computed values by clicking on any node, Gauss region, or flux section. Then prepare the results for reporting by adding labels, axes, and pictures, or export the results into other applications such as Microsoft Excel for further analysis.

In this research, the analysis of seepage and pore-water pressure distribution is done using this model. The model inputs used for this research using SEEP/W model are the pressure and material properties (hydraulic conductivity).

Table 2.2 Loading Conditions and Boundary Conditions

S.No.	Analysis methods	Loading conditions	Boundary conditions
1	Seepage Analysis	Steady state seepage Steady state seepage with earthquake	On upstream side total head
			At the downstream there is horizontal filter. The granular material is highly permeable; This implies that there is no head loss in the drain relative to the small amount of seepage that will come through the low permeability embankment material. The total head around the rock toe perimeter and beyond is therefore assumed to be the elevation of the original ground level (OGL).

a. Model Applications

SEEP/W can model problems including:

- ❖ Dissipation of excess pore pressure after reservoir drawdown
- ❖ Changes in pore-water pressure conditions within earth slopes due to infiltration of precipitation
- ❖ Mounding of the groundwater table beneath water retention structures such as lagoons and tailings ponds
- ❖ Effect of subsurface drains and injection wells
- ❖ Drawdown of a water table due to pumping from an aquifer
- ❖ Seepage flow quantities into excavations

b. SEEP/W Integrated with Other Applications

Dissipate excess pore-water pressures generated by SIGMA/W or QUAKE/W. Excess pore-water pressures generated by static loading (e.g., fill placement) or by dynamic motion during an earthquake can be brought into SEEP/W to study how long it takes to dissipate the excess pressures. Using finite element computed pore-water pressures in SLOPE/W makes it possible to deal with highly irregular saturated / unsaturated conditions or transient pore-water pressure conditions in a stability analysis. For example, we can analyze changes in stability as the pore-water pressure changes with time. Use SEEP/W data inside a CTRAN/W model for contaminant transport or a TEMP/W model for convective heat transfer analysis.

c. Pore Water Pressure Prediction

Every dam must be subjected to the filling test to ensure its safety performance. For an embankment dam, it is imperative to monitor the behavior of its pore water pressures particularly in the early stage of its service life span of first reservoir filling. However, the safety of the dam is not proven until it is subjected to the first filling to its top water level.
The followings are methods for the determination of pore pressures.

a. Phreatic Surface Method

Pore water pressures for steady-state seepage loading conditions can be estimated as hydrostatic pressures below the steady-state phreatic surface without introducing significant error. The steady-state phreatic surface can be estimated following established procedures developed by Casagrande [10], Pavlovsky [11], Cedergren [12], or others. In general, pore water pressures estimated from the phreatic surface method are conservative for zoned embankments; however, this method may underestimate the values for some special loading conditions such as infiltration of precipitation, artesian pressures in foundation, etc. Other methods of evaluating pore pressures should be used in such cases. It is acceptable to have multiple phreatic surfaces in a zoned embankment, one for each of the zones in the embankment and its foundation.

The phreatic surface method can also be used for determining pore pressures under rapid drawdown conditions. The phreatic surface from the steady seepage condition is modified in accordance with the following conservative assumptions:
(1) Pore pressure dissipation as a result of drainage does not occur during drawdown in impervious materials and (2) the water surface is lowered instantaneously from the top of active conservation water surface to the top of inactive conservation capacity water surface. The phreatic surface may be assumed to follow the upstream surface of the embankment. For embankments with semi pervious shell materials, partial dissipation of pore pressures may be assumed in the shell material.

The phreatic surface method is not appropriate for determining pore pressures under end of construction or during construction loading conditions.

b. Graphical Flow Net Method

Under steady-state seepage conditions, flow net methods of analysis are used on transformed sections of the embankment and foundation to determine pore pressures. The values of horizontal to vertical permeability ratios depend on the method of compaction of embankment materials and/or geologic history of the foundation materials.

c. Numerical Methods

Numerical methods for determining pore pressures are excellent tools for rapid drawdown and steady-state seepage loading conditions for complex geometric conditions and are the only way to compute pore pressures in three-dimensional space. However, the added degree of sophistication is not necessary in most cases. Finite element, finite difference, and boundary element are some of the well-known numerical methods that are used to determine pore pressures.

For estimating pore water pressure during rapid drawdown, numerical procedures that reflect the influence of dilatancy on the pore water pressure changes are based on stress changes during drawdown. These procedures are described in reference [5].

Permeability of all materials in the embankment and foundation must be known in order to get an accurate estimate of pressures and flow. If necessary, numerical methods should be considered in the final phase of design.

d. Field Measurement (Instrumentation) Method

The development of pore pressures during construction in either the foundation or in the embankment depends upon the soil properties and the amount of consolidation occurring during construction. Pore pressure observations made during construction should be compared with the predicted magnitudes of pore pressures for effective stress analysis to ensure that the actual pore pressures do not rise to a level that will cause instability.

e. Hilf's Method

A detailed procedure for predicting a total stress versus pore water pressure curve from the results of a few laboratory consolidation tests and a large number of field percolation-settlement tests is given by Hilf. The procedure can be adapted to estimate pore water pressures during construction stages.

The prediction of pore water pressures in fill dams in the early stage of first filling reservoir particularly poses some difficulty as the embankment fill is in unsaturated condition immediately after construction.

2.6 Hydraulic Conductivity

Hydraulic conductivity is a property of both the soil particles and pore fluid comprising the porous medium, and is dependent on particle size and shape, void ratio, amount and mineralogy of the fine fraction, degree of saturation, and temperature [22]. Hydraulic conductivity can be described for a saturated uniform soil of grain Diameter *d* [m] by equation 2.3 below, where μ is dynamic fluid viscosity [Pa.s], *k* is the intrinsic Permeability of the soil [m^2], and c is a coefficient of proportionality that describes the grain size distribution, roundness and packing.

$$K = (k\rho_w g)/\mu \qquad (2.3)$$

Where, $k = cd^2$

Table 2.3 Typical Hydraulic Conductivity Values (Domenico and Schwartz, 1998).

Material	K
Gravel	$3\times10^{-4} – 3\times10^{-2}$
Coarse sand	$9\times10^{-7} – 6\times10^{-3}$
Medium sand	$9\times10^{-7} – 5\times10^{-4}$
Fine sand	$2\times10^{-7} – 2\times10^{-4}$
Silt, loess	$1\times10^{-9} – 2\times10^{-5}$
Glacial till	$1\times10^{-12} – 2\times10^{-6}$
Clay	$1\times10^{-11} – 5\times10^{-9}$
Unweathered marine clay	$8\times10^{-13} – 2\times10^{-9}$
Limestone, dolomite	$1\times10^{-9} – 6\times10^{-6}$
Sandstone	$3\times10^{-10} – 6\times10^{-6}$
Unfractured igneous an metamorphic rocks	$3\times10^{-14} – 2\times10^{-10}$

As porosity is a function of the grain packing arrangement, many researchers have attempted to define the coefficient c in Equation 2-3 in terms of porosity. The Kozeny- Carman equation [25], relates hydraulic conductivity *K* [m/s] to a representative mean grain size d_m [m], which is not strictly defined. This relation was derived from experiments conducted on uniform sands at various densities.

$$K = \frac{k\rho_w g}{\mu[n^3/(1-n)^2](d_m^3/180)} \qquad (2.4)$$

One of the most important parameter in embankment dam analysis is the hydraulic conductivity or the term is sometimes named as coefficient of permeability. The hydraulic conductivities of the various zoning parts of the embankment dam vary based on the engineering requirements.
The clay test result from the Kesem dam design report reveals that the hydraulic conductivity detected at two clay borrow sites is ranging between 1.14×10^{-8} and 1.3×10^{-7}cm/s, 4.88×10^{-7} and 2.74×10^{-6}cm/s, respectively.

The hydraulic conductivity (seepage coefficient) value for the Kesem dam core is 6.0710^{-6} cm/s [9]. The hydraulic conductivity test was done in the central laboratory in Addis Ababa. The site monitoring work is mainly based on compaction. The shell and other freely drainage materials can be checked in the site with trial embankments. Besides this, monitoring of moisture content and other compaction results are carefully analyzed whether it attains the required standard or not. The overall conductivity monitoring as specified in laboratory result.

2.7 Instrumentation and Dam Surveillance

Records of instrumentation observations are important in determining changes in pore water pressure, deformations, and settlements. The data, when summarized and evaluated, are useful in substantiating design assumptions and thus in verifying stability during construction, designing modifications, and additions to structures, or determining.

Observations of seepage quantities from relief wells, toe drains, seepage galleries, and other seepage control installations should be recorded on appropriate locally developed forms for evaluation at the project and district levels. Unusual seepage conditions should be reported immediately to the district office along with available observational data for evaluation of the effect of existing conditions on the safety of the dam.

Various types of piezometers are usually installed in an embankment dam so that they compensate one another's disadvantages [5]. Among widely used types are open standpipe and vibrating wire piezometers. While open standpipe piezometers are simple durable devices with relatively high reliabilities, they need to transmit a large amount of water before they can reflect a certain change in pore water pressure. On the other hand, vibrating wire piezometers are hydro electrical devices, which operate based on a vibrating wire transducer with no need for transmitting water. However, during the dam construction, filling and compaction of earth material may expose the transducer cell to an enormous increase in the total stress. If the cell is not rigid enough, then its deformations will change the wire tension, in which case, the piezometer readings would not be reliable [6].

Piezometer readings are usually utilized to model and analyze the behavior of pore water pressure in an embankment dam. Pore water pressures may be modeled under a steady state or transient condition, depending on the situation. For example, if the reservoir level remains constant for a long period of time, one may assume a steady state for pore water pressure. On the other hand, in order to model pore pressures following dam impoundments, it seems necessary to perform a transient analysis. In any case, whether the pore pressure has reached a steady state or not is not always a simple question to answer. Monitoring and modeling pore pressures in dams are common approaches taken to answer such questions [7].

The initial reservoir filling is defined as a deliberate impoundment to meet project purposes and is a continuing process as successively higher pools are attained for flood control projects. The initial reservoir filling is the first test of the dam to perform the function for which it was designed. In order to monitor this performance, the rate of filling should be controlled to the extent feasible, to allow as much time as needed for a predetermined surveillance program including the observation and analysis of instrumentation data [21].

3. METHODOLOGY

3.1 Introduction

Kesem Dam and irrigation project is located in Afar Regional State, Ethiopia. The ground distance is 215 km from Addis Ababa, in the middle Awash valley, which covers the Kesem sub basin.

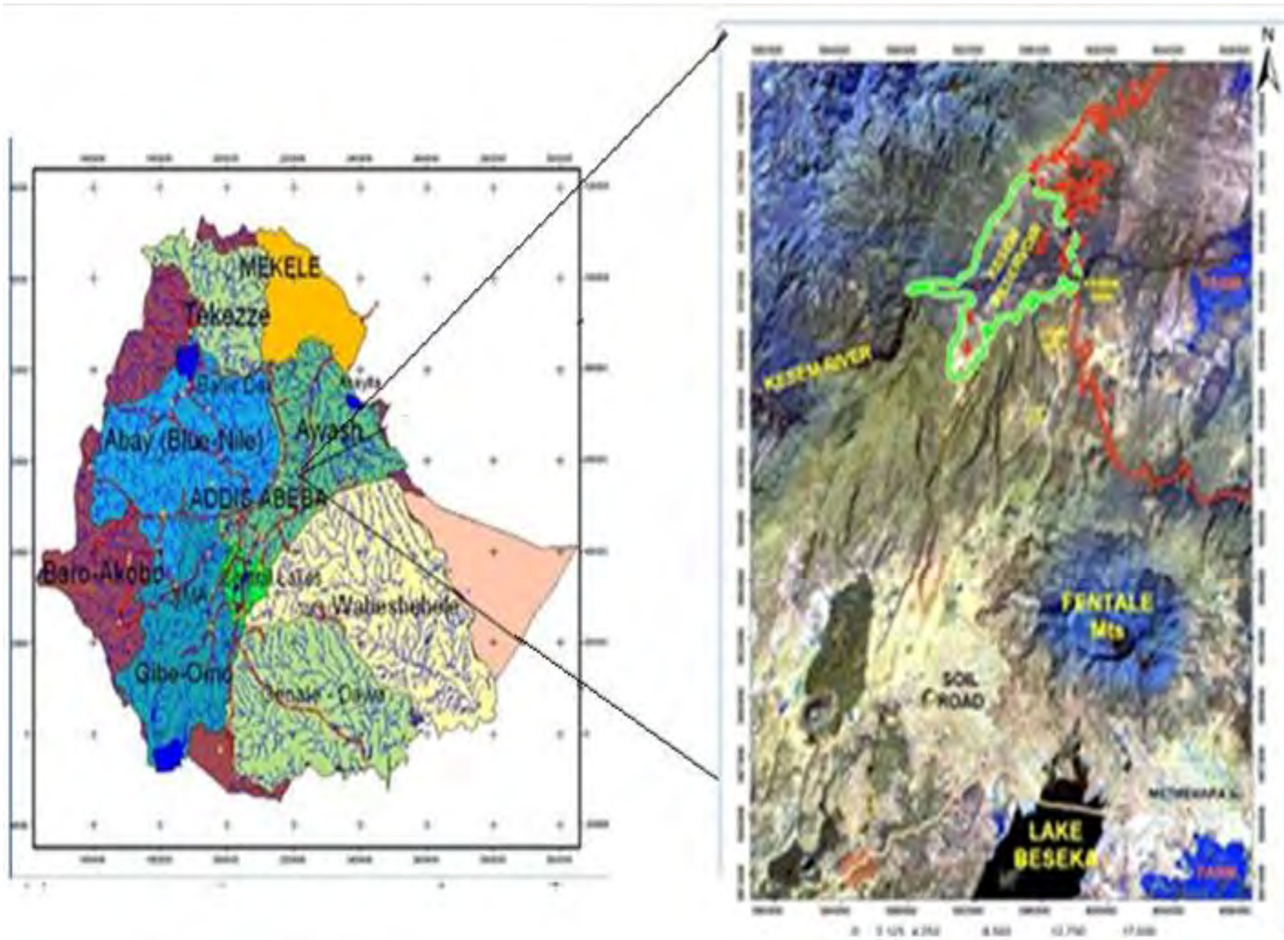

Figure 3.1 Kesem Dam Location

3.2 Data Collection

The following data were used in this thesis

- Pore pressure
- Material properties of dam
- Hydraulic parameters (permeability)
- Construction drawing
- Reservoir water level

Required data were collected from Water Works Design and Supervision Enterprise (WWDSE), Water Works Construction Enterprise (WWCE) and from Kesem dam site.

3.2.1 Primary Data

The primary data was collected from Kesem dam site. During site visit cross checking of secondary data that already have been collected from WWDSE and WWCE and checking of the location of some control points on the site was done with;

- Visual inspection of the dam and locations of piezometers.
- Interview of the resident engineer, hydro geologist and site engineers.
- Collect pictures that show the reservoir water level, the dam body and its appurtenant structures with digital camera.

3.2.2 Secondary Data

Secondary data were collected from Water Works Design and Supervision Enterprise (WWDSE) and Water Works Construction Enterprise as well as from Kesem dam site. The raw data on pore water pressure, reservoir water level, instrument location and design drawings are obtained from the above mentioned organizations.

- Dam cross sectional design and Geological report data were collected from the Water Works Design and Supervision Enterprise (WWDSE).
- Piezometric reading data from dam site.

- Hydraulic conductivity laboratory test result from the dam site.
- Reservoir Water level from the dam site recorded data.

3.3 Modeling Approach

In construction quality monitoring of embankment dams, conductivity of the different zoning parts have significant role for pore pressure prediction. For Kesem dam, the pore water pressure data was collected from the dam site. At the same time reservoir water level data were taken. Representative piezometers were selected from wider dam section at five points.

3.3.1 Geo Slope International (GeoStudio2004/SEEP/W)

GeoStudio2004 is finite element method which is now commonly adopted for modeling civil engineering structures mainly:

- Dams and levees
- Reinforced walls and slopes
- Excavation and open pit mines
- Roads, bridges and embankments
- Earthquake deformation

It is a powerful tool for the analysis of many geotechnical structures. The sub program of GeoStudio2004 named SEEP/W is finite element cad software used in seepage modeling in embankment dams, ground water seepage analysis and for excess pore water pressure dissipation problems.

In order to design the chimney and horizontal filter seepage analysis through the dam only and through the dam and the foundation also required.

Besides, the computed phreatic surface is used to set up the pore water pressure line in the stability analysis of the dam. For this research, the result from SEEP/W analysis is used to determine the phreatic surface line and pore water pressure at different piezometric locations.

3.3.2 Analysis of Data using Geo-studio

The model inputs used for this research using SEEP/W model are the pressure and material properties (hydraulic conductivity).

Hydraulic conductivity is a property of both the soil particles and pore fluid comprising the porous medium, and is dependent on particle size and shape, void ratio, amount and mineralogy of the fine fraction, degree of saturation, and temperature [22].

Hydraulic conductivity in an embankment dams is the most critical parameter which influence the amount of water in the earthen embankment and at the same time affects the stability of the dam due to excessive seepage through the dam body and the foundation. For this study, the hydraulic conductivity of the embankment section is considered since the scope of the thesis is on the embankment section of the dam.

In this research the finite element method available in SEEP/W was employed to simulate 2-D steady state seepage analysis in the embankment dam. The finite element modeling system selected is 2-dimensional due to:

- Simplicity
- To be more accurate based on available data

Prior to simulation, the dam was analyzed for steady-state seepage conditions, by taking the reservoir water level at different level taking different hydraulic conductivity values of the dam. Outcomes of the steady-state seepage analysis were then used to determine the location of phreatic lines on the respective reservoir water level.

a. Determination of Phreatic Line

Phreatic line / seepage line / Saturation line is the line at the upper surface of the seepage flow at which the pressure is atmospheric.

It is hardly possible to locate the position of the phreatic line in equation form for zoned embankment dams. Most of the researches done on embankment dams related to the location of phreatic line are for homogeneous embankment dams. Location of phreatic line and calculation of seepage for homogenous embankment dams was determined previously [18]. For rock fill dams and other zoned embankment dams determination of seepage through the dam body and determination of phreatic line is done using finite elements. Among the different finite element methods, GeoStudio 2004(SEEP/W) is used for this thesis.

b. Boundary Conditions

Boundary conditions are essential to solve the SEEP/W finite element problems. In seepage analysis with SEEP/W, there are two fundamental boundary conditions namely, the head boundary condition and the flux boundary condition.

Thus, in modeling of Kesem dam, the head boundary condition have been used from the recorded reservoir water level values at 896.5m, 897.20m, 898.28m, 902.89m, 905.48m, 906.66m and 907.57m. The water level in the reservoir was taken as head boundary condition and the embankment dam was modeled for the steady state condition. After the result of the model, the location of phreatic line for the above head boundary conditions was determined.

The locations of piezometers were collected from the design document inside the dam body which are on the representative wider section of the dam.

There are totally 30 piezometers on four sections in Kesem dam for measuring of pore pressure. In this thesis, piezometric location at sec 3-3 were selected due to the following reasons

- It is nearer to the dam axis
- It is at the deepest location
- The critical section is the core because of the higher permeability variation at the upstream and downstream of the core.

After running the model, the pore water pressures was obtained on each instrument locations inside the dam by tracing the x-y coordinates.

3.3.3 Multiple Linear Regression (MLR)

The pore water pressure obtained from analysis result of SEEP/W and the actual recorded pressure values at different selected piezometric locations were used in Multiple Linear Regression (MLR) as an input. The correlation between recorded and simulated results of pore water pressure was analyzed using multiple linear regression. The coefficients of regression were obtained for each instrument labeled as $P_{3\text{-}6}$, $P_{3\text{-}7}$, $P_{3\text{-}8}$, $P_{3\text{-}9}$, $P_{3\text{-}10}$, and $P_{3\text{-}11}$.

Multiple linear regressions is an extension of linear regression and is used to represent the relationship between a dependent variable and several independent variables. In this research for the six distinct instrumental readings, measured pore pressure was taken at a given water level elevation in the reservoir. The general form of multiple linear regressions can be written as follows

$y = a_o + a_1x_1 + a_2x_2 + a_3x_3 + \ldots\ldots\ldots\ldots\ldots\ldots a_nx$ (3.1)

Where, $a_0, a_1, a_2.a_3, \ldots.a_n$ are coefficients

and $x_1, x_2, x_3, \ldots\ldots\ldots x_n$ are simulated results

y is the measured value

The measured values and the results obtained from the analysis of SEEP/W relationship was studied after obtaining calibrated MLR coefficients. The solved results of the equations using MLR yields calibrated MLR coefficients and other statistical values.

After taking calibrated MLR coefficients, and observing the nature of the correlation coefficient from the statistical value the applicability of construction quality monitoring using pore water pressure was assessed.

3.4 Conceptual Model

At first, different hydrogeological parameters (K_1, K_2, K_3, K_4, K_5) are assigned for the dam core section. Then a 2-D seepage flow analysis model (SEEP/W) is used to estimate the pore water pressure at the sensors ((P_{3-6} , P_{3-7} , P_{3-8} ,P_{3-10} ,P_{3-11}). This model uses the water level inside the reservoir and the hydraulic conductivities as its input for the prediction of the pore pressures. Since, the hydraulic conductivity values seldom result in appropriate pore pressure prediction, a second phase of modeling (multiple linear regression modeling) is used for accurate prediction of pore pressures. The multiple regression model used the SEEP/W model outputs as an input to predict the measured pore pressures at each sensor location. This finally results in regression coefficients for further monitoring of embankment dam safety.

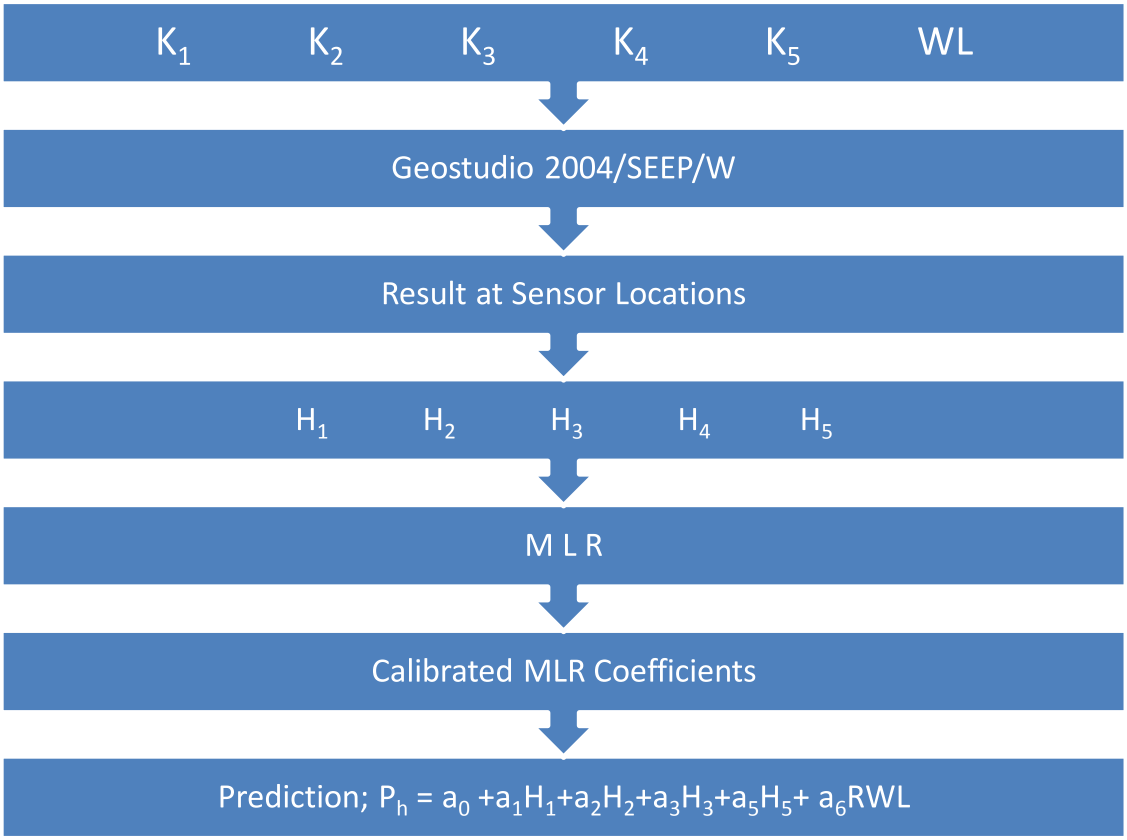

Figure 3.2 Methods of Modeling

4. RESULTS AND DISCUSSIONS

Monitored piezometric data at different elevations were taken and reservoir water level at the respective dates was also used for the analysis. The graph of date versus water level as well as date versus different piezometric reading is plotted. From this, the trend of the graph was observed for each pressure cell. Some of the piezometric readings are negative; this is because pressure head at this location is below the elevation head of the location. During the impoundment, there is fluctuation in water level of the reservoir. This might be due to various reasons. One of the main reasons is due to seasonal inflow variation, that is during the rainy seasons(summer) there is rapid increase whereas in dry seasons(winter) there is decline in water level due to water release from the reservoir and high evaporation Ten months reservoir water level data is available for the analysis. The monitored available data are from December 2012 to August 2013. On the other hand, the piezometric data available varies depending on the instrument locations. On some of the piezometers there is recorded data as long as 17 months.

The piezometers located on the upstream section of the dam are more important for the analysis than the piezometers located on downstream section of the dam due to two main reasons:

- The reservoir water level is near to piezometers
- There is no downstream water level

Results of this study are presented in two sections. First, pore pressures monitored by piezometers installed at different elevations in the core are presented and discussed. Second, the results of modeling pore pressures under steady state conditions are described and compared with certain monitored data.

4.1 Pore Pressure Monitoring

Five hydraulic conductivity values are selected. These values are for the impervious (core) part since modeling is focused on the core. Two values are higher than the design conductivity value and the remaining two are less than the design value. This is because the designed values has seldom results in the measured pore pressures for a given reservoir level.

For a given reservoir water level, the five hydraulic conductivity values are assigned taking the permeability used in the design as a base.

Construction of the dam has been almost completed. Following construction of the dam body, impoundment of the reservoir and monitoring pore pressure heads in the dam body started. In this study, monitored heads in section 3-3, were collected starting from the period of the first reading 21/02/2012 to the last reading 8/10/2012 following the dam construction and impoundment, are presented and discussed.

I. *Piezometers installed at el. 862.3m (in the dam body):* A total of three piezometers (P_{3-6}, P_{3-7} and P_{3-8}) were installed at this elevation. They were numbered sequentially from the upstream to the downstream face of the core. Table 4.1.shows the readings of available piezometers as well as the reservoir water level. The reservoir level varies between early and late dam impoundments.

Table 4.1 Piezometric Readings at el. 862.3m

WL(m)	P3-6	P3-7	P3-8
	Measured (m)	Measured(m)	Measured(m)
896.5	861.76	861.47	862.89
897.20	862.23	861.74	862.32
898.28	861.71	862.51	862.23
902.89	870.24	866.21	1383.00
905.48	865.61	864.13	864.07
906.66	864.27	863.71	862.77
907.57	863.46	863.45	1642.86

In this period, some piezometers showed heads higher than the reservoir level. It is postulated that a high pore pressure induced by construction existed in the core, which was dissipating gradually. Head dissipation was slow, especially near the upstream face of the core (P_{3-6}, P_{3-7}), due to the low hydraulic gradient and conductivity there. A faster dissipation, observed in piezometer P_{3-8} in the same period, was attributed to its location being close to the highly conductive downstream filter and high gradient there.

During the impoundment of the dam an increase in the reservoir level (from el. 896.5 to el. 907.57) occurred in eight month period. In response to this impoundment, piezometers near the upstream face of the core responded slow compared to the downstream face, so that $P_{3\text{-}6}$ and $P_{3\text{-}7}$ showed increases of 1.7 and 1.98 meters in their water levels, respectively. This behavior was expected due to reservoir water level increase.

II. Piezometers installed at el. 890.3: Monitored heads at two piezometers installed at this elevation ($P_{3\text{-}9}$ and $P_{3\text{-}10}$) are shown on Table.4.2. As in the previous elevation, the general trend during the varying reservoir level is that piezometers show higher heads near the upstream and lower ones near the downstream face of the core.

Table 4.2 Piezometric Readings at el. 890.3m

WL(m)	P3-9	P3-10
	Measured(m)	Measured(m)
896.50	889.51	886.98
897.20	889.51	886.97
898.28	884.52	892.35
902.89	868.30	897.51
905.48	870.13	899.89
906.66	874.90	896.31
907.57	877.50	894.99

Moving downstream, $P_{3\text{-}9}$ to $P_{3\text{-}10}$ exhibited slower responses with fewer total increases in their water levels, respectively. In general, the behavior of the pore pressure at this elevation was similar to that explained at el. 862.3.

II. Piezometers installed at el. 916.3: $P_{3\text{-}11}$ was the only sensor installed at this elevation Table 4.3 shows the monitored heads obtained from this piezometer.

Table 4.3 Piezometric Readings at el. 916.3m

WL(m)	P3-11
	Measured(m)
896.50	893.01
897.20	893.65
898.28	894.65
902.89	912.08
905.48	912.24
906.66	912.28
907.57	912.33

Its' general behavior is similar to those installed at lower elevations except for the fact that at this elevation most of the readings in this piezometer shows heads which are higher than the reservoir level. As discussed before, the high head at this piezometer was induced because of the higher installed elevation of the piezometer and the lower reservoir water level. During the entire period of the study, piezometers installed at 916.3 showed negative pore water pressures. This was attributed to the reservoir level always remaining lower than this elevation during the study.

4.2 Modeling Results

After analysis of Kesem dam using the Geo-studio2004 (SEEP/W) model, the research used the first reservoir water level of 896.5m. The water level in the reservoir was taken as constant head boundary condition. The location of phreatic line determined for the above head boundary condition is shown in Figure 4.1.

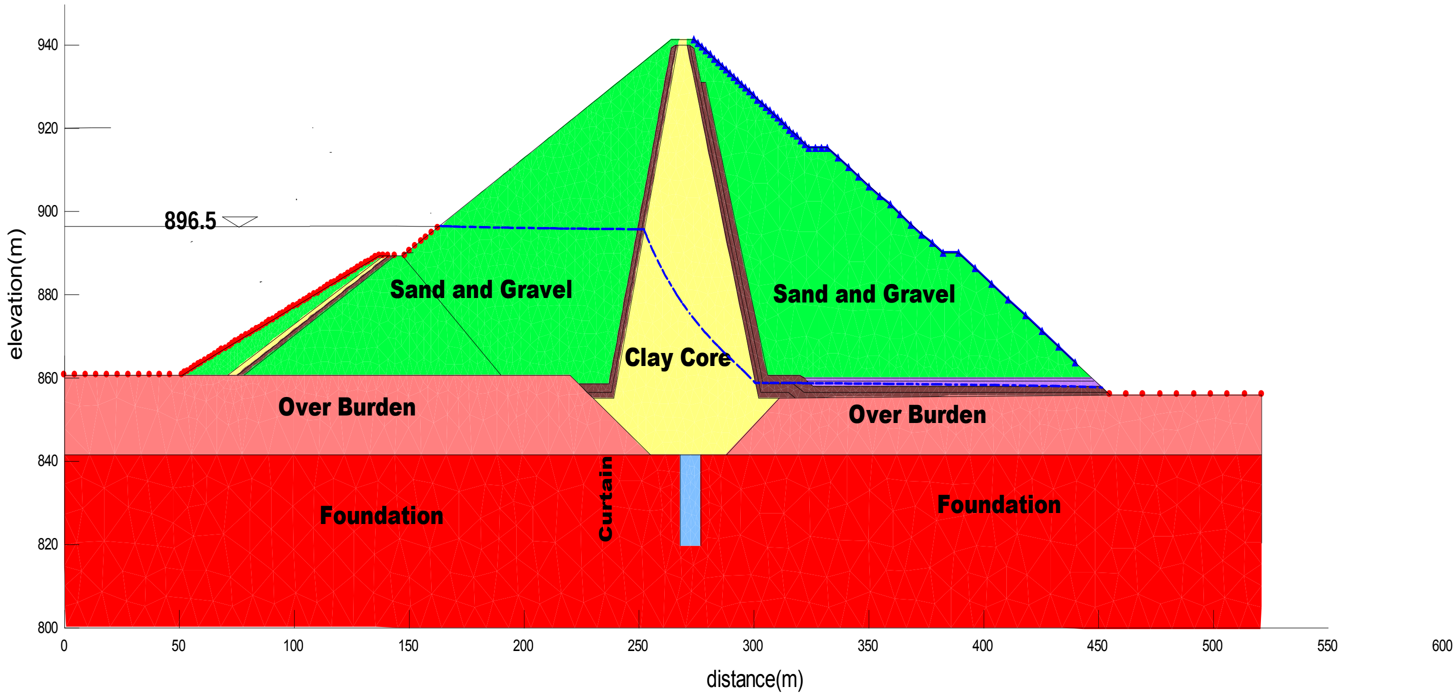

Figure 4.1 Phreatic Line for 896.5 WL

Then from the SEEP/W model analysis result, the pressure heads obtained at the nodes representing the different pressure monitoring sensors is as shown in Table 4.4. Note: each hydraulic conductivity value results in different pressure heads.

Table 4.4 Total Head Versus K-values at 896.5 WL

K-values (cm/s)	P_{3-6}	P_{3-7}	P_{3-8}	P_{3-9}	P_{3-10}	P_{3-11}
	Total Head(m)					
6*10-4	887.27	883.95	881.37	886.33	882.41	884.93
6*10-5	891.84	883.69	877.31	891.10	879.63	889.67
6*10-6	894.32	883.21	874.81	894.09	877.84	893.03
6*10-7	894.60	882.98	874.40	894.59	877.54	893.59
6*10-8	894.62	882.94	874.35	894.64	877.50	893.65

In the same way for each hydraulic conductivity values and reservoir water levels of 897.20,898.28,902.89,905.48,906.66 and 907.57 the phreatic line and pressure heads obtained at the six sensor locations of the dam are as shown in the Figures 4.2 -4.7 and Tables 4.5-4.10, respectively.

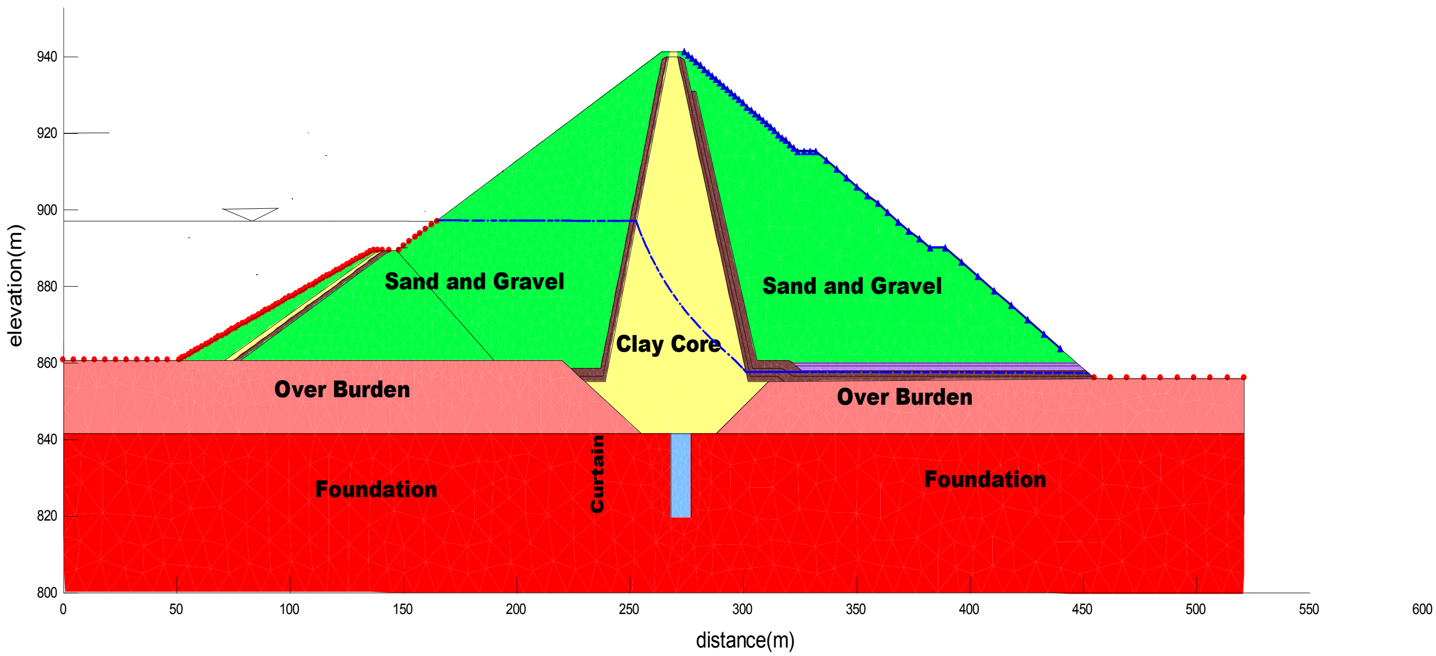

Figure 4.2 Phreatic Line at 897.2 WL

Table 4.5 Total Head Versus K-values at 897.2 WL

K-values (cm/s)	P_{3-6}	P_{3-7}	P_{3-8}	P_{3-9}	P_{3-10}	P_{3-11}
	Total Head(m)					
6*10-4	886.44	883.21	880.7	885.52	881.72	884.16
6*10-5	886.44	883.21	880.7	885.52	881.72	884.16
6*10-6	893.64	882.73	874.49	893.41	877.46	892.37
6*10-7	893.94	882.52	874.09	893.92	877.17	892.94
6*10-8	893.96	882.48	874.05	893.98	877.14	893.00

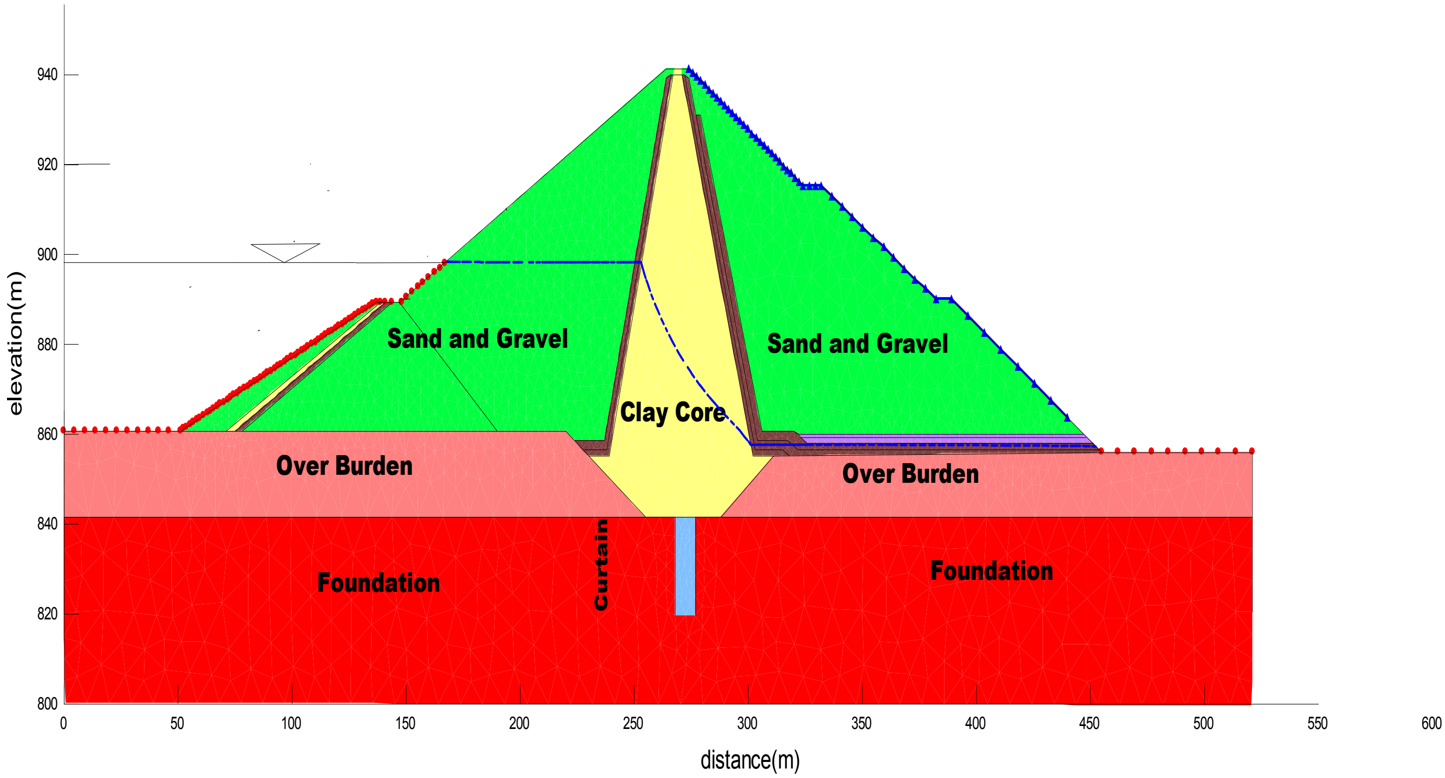

Figure 4.3 Phreatic Line at 898.28 WL

Table 4.6 Total Head Versus K-values at 898.28 WL

K- values (cm/s)	P_{3-6}	P_{3-7}	P_{3-8}	P_{3-9}	P_{3-10}	P_{3-11}
	Total Head(m)					
6*10-4	888.37	884.93	882.26	887.41	883.35	885.95
6*10-5	892.93	884.52	877.94	892.17	880.33	890.70
6*10-6	895.36	883.94	875.31	895.12	878.42	894.03
6*10-7	895.62	883.68	874.87	895.61	878.10	894.58
6*10-8	895.64	883.64	874.82	895.66	878.06	894.64

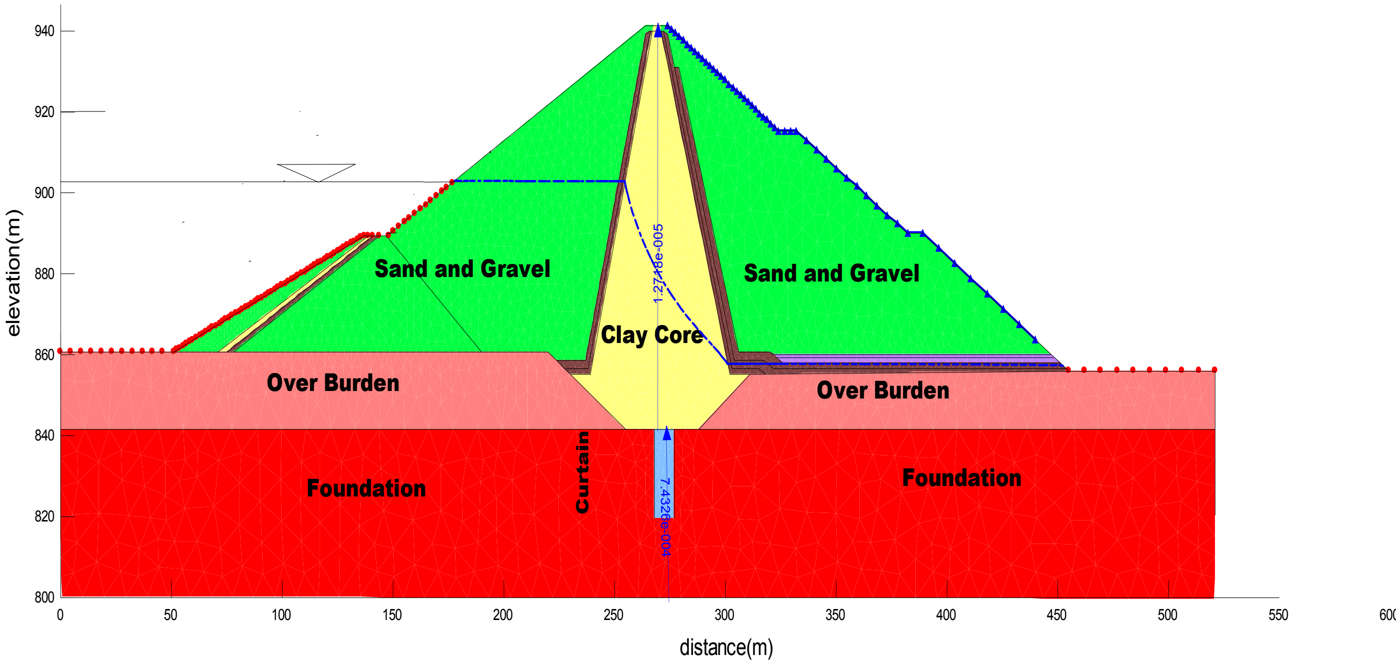

Figure 4.4 Phreatic Line at 902.89 WL

Table 4.7 Total Head Versus K-values at 902.89 WL

K-values (cm/s)	P_{3-6}	P_{3-7}	P_{3-8}	P_{3-9}	P_{3-10}	P_{3-11}
	Total Head(m)					
6*10-4	893.13	889.17	886.10	892.04	887.36	890.38
6*10-5	897.56	888.05	880.62	896.72	883.35	895.06
6*10-6	899.77	887.03	877.41	899.51	880.88	898.30
6*10-7	899.98	886.69	876.89	899.97	879.72	898.83
6*10-8	899.99	864.64	876.83	900.02	880.43	898.88

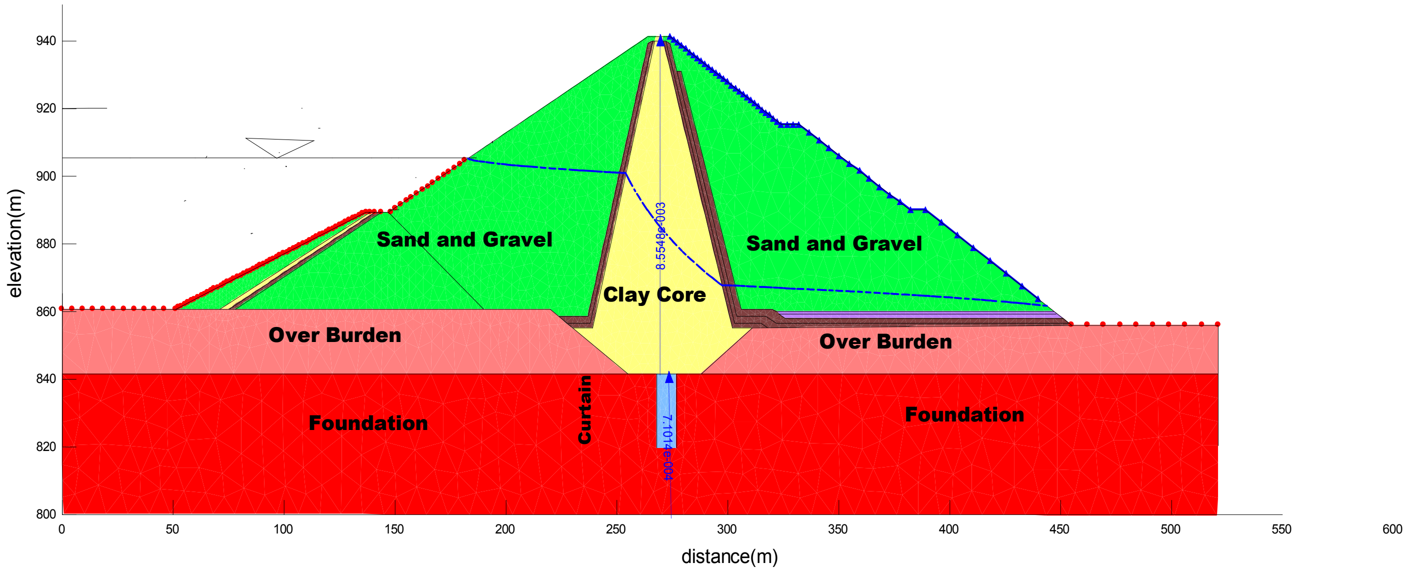

Figure 4.5 Phreatic Line at 905.48 WL

Table 4.8 Total Head Versus K-values at 905.48 WL

K-values (cm/s)	P_{3-6}	P3-7	P_{3-8}	P_{3-9}	P_{3-10}	P_{3-11}
	Total Head(m)					
6*10-4	895.79	891.54	888.25	894.64	889.61	892.87
6*10-5	900.15	890.03	882.12	899.26	885.03	897.50
6*10-6	902.24	888.76	878.58	901.98	882.27	900.69
6*10-7	902.43	888.38	878.01	901.21	881.81	901.21
6*10-8	902.43	888.32	877.95	902.46	881.76	901.26

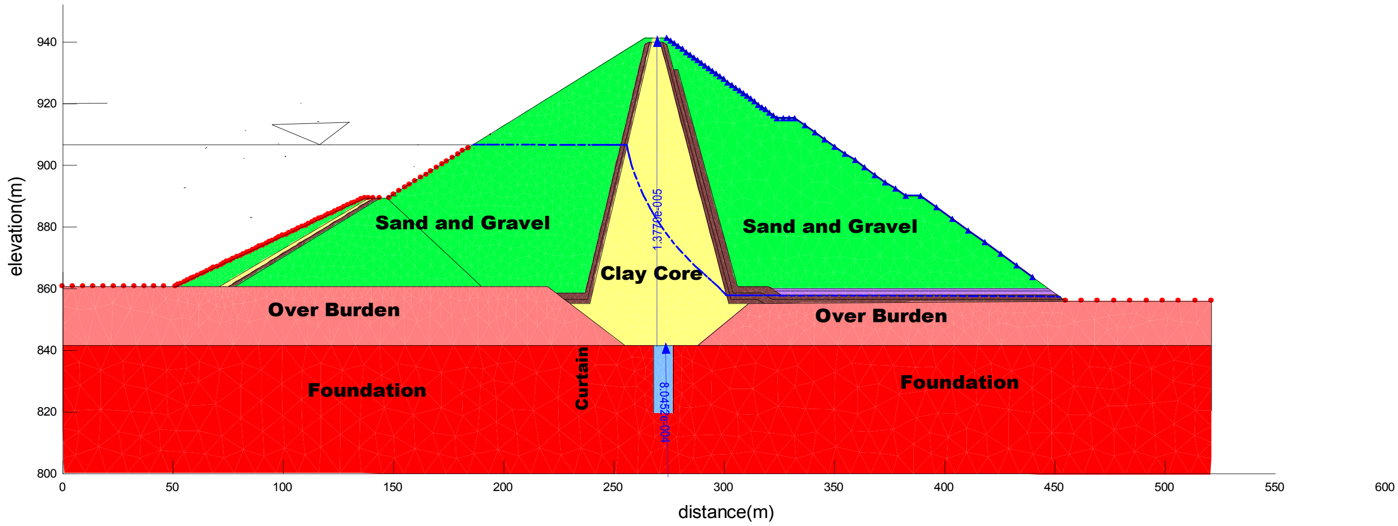

Figure 4.6 Phreatic Line at 906.66 WL

Table 4.9 Total Head Versus K-values at 906.66 WL

K-values (cm/s)	P_{3-6}	P_{3-7}	P_{3-8}	P_{3-9}	P_{3-10}	P_{3-11}
	Total Head(m)					
6*10-4	897.05	892.68	889.28	895.89	890.69	894.06
6*10-5	901.35	890.94	882.82	900.44	885.82	898.64
6*10-6	903.37	889.55	879.12	903.10	882.90	901.78
6*10-7	903.54	889.15	878.53	903.53	882.42	902.29
6*10-8	903.55	889.08	878.46	903.57	882.37	902.35

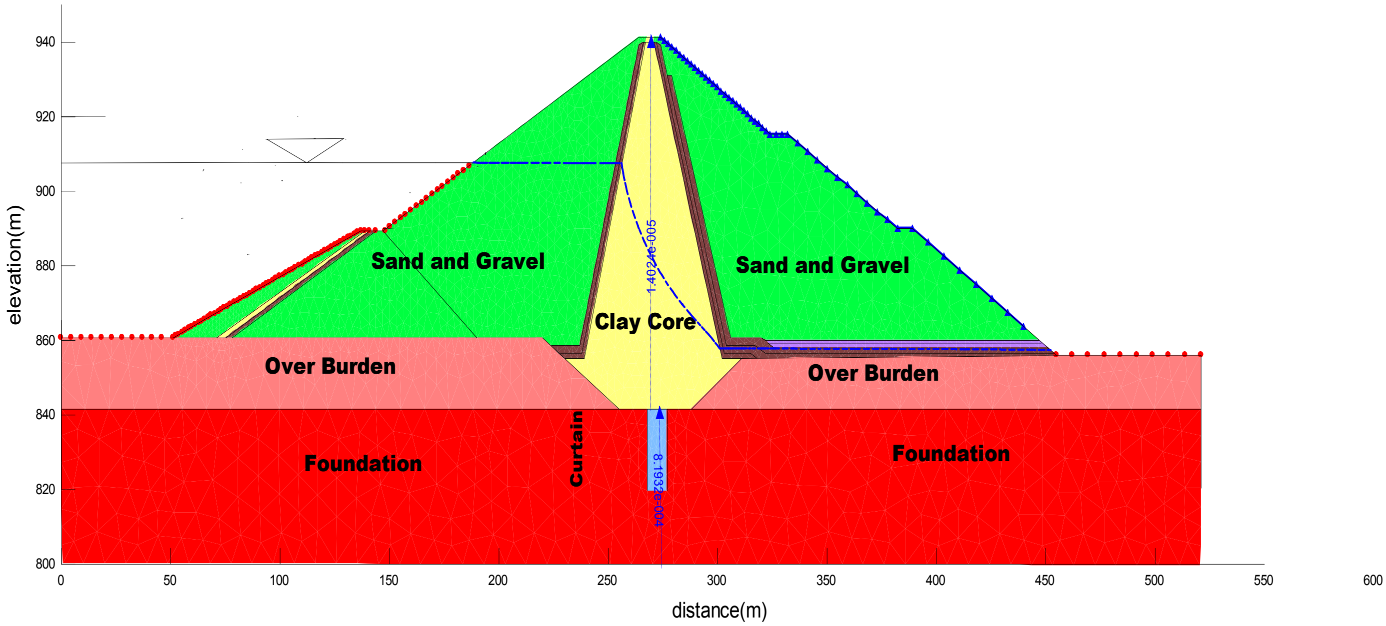

Figure 4.7 Phreatic Line at 907.57 WL

Table 4.10 Total Head Versus K-values at 907.57 WL

K-values (cm/s)	P_{3-6}	P_{3-7}	P_{3-8}	P_{3-9}	P_{3-10}	P_{3-11}
	Total Head(m)					
6*10-4	898.11	893.62	890.14	896.93	891.59	895.06
6*10-5	902.31	891.68	883.38	901.4	886.45	899.56
6*10-6	904.25	890.17	879.54	903.98	883.39	902.63
6*10-7	904.40	889.74	878.93	904.39	882.89	903.13
6*10-8	904.40	889.68	878.86	904.43	882.84	903.18

According to this research modeling approach the results from SEEP/W model (Table 4.4-4.10) are used as an input to a multiple linear regression analysis of the form.

$P_h = a_0 + a_1P_{h1} + a_2P_{h2} + a_3P_{h3} + a_4P_{h4} + a_6P_{h5} + a_6RWL$ (3.2)

Where P_{h1} is the pressure head at sensor for K_1

P_{h2} is the pressure head at sensor for K_2

P_{h3} is the pressure head at sensor for K_3

P_{h4} is the pressure head at sensor for K_4

P_{h5} is the pressure head at sensor for K_5

RWL Reservoir Water Level

P_h pressure head to be determined

In multiple regression analysis the regression coefficients a_0 a_1……a_6 are obtained by using the measured pressure heads in place of P_h. The inputs to the MLR analysis are attached in the appendix Tabe 6.2

After the analysis result of SEEP/W relationship between the measured and simulated result was studied using multiple regression method. The results of the regression coefficients and R^2 values obtained by applying the multiple linear regression equation for each piezometric levels are shown in Table 4.11

Table 4.11 Results of MLR

Reg. coef.	P_{3-6}	P_{3-7}	P_{3-8}	P_{3-9}	P_{3-10}	P_{3-11}
a_o	-235318.176	-238908.164	14996.765	-240486.282	-468949.030	-66641.321
a_1	872.361	484.821	-109.291	4486.724	1285.924	7343.056
a_2	221.448	47.605	-44.398	332.715	-2.526	551.329
a_3	-473.685	-260.437	84.474	-1566.763	-179.410	-2041.927
a_4	2848.859	290.227	-22.699	23.820	-15.723	-4625.721
a_5	1585.800	215.963	48.646	163.370	39.653	-179.865
a_6	-4776.304	-498.562	26.537	-3157.672	-579.530	-966.391
R^2	1	1	1	1	1	1

Construction quality monitoring techniques of embankment dams using pore water pressure was done in this thesis by using the relationship between the result from the model and the recorded values of the piezometric readings. The results of the pore water pressure in the piezometric areas from the model are almost the same as the result that was obtained from the recorded data. This is proved using the multiple regression equation correlation coefficient of R^2 is approximately 1 for each piezometric area. This result shows the techniques of construction monitoring used is good.

For different reservoir water level, we can predict the pore water pressure that nearly gives equal value to the model value on the piezometric area.

The method of monitoring of embankment dam by pore water pressure can give a good result when the values from the model output is approximately the same as the result obtained from the instrument readings. Otherwise it gives not good construction monitoring techniques that should be an indicative to use other techniques of monitoring to improve the dam safety.

To get best result the piezometric instruments located on the upstream section is the first choice because of no tail water on the downstream section of the dam and the core section is much sensitive part due to impervious section of the dam.

4.3 Model Application

For any reservoir level X, SEEP/W will compute five piezometric head (P_h) values at any of the sensors location for the five hydraulic conductivity values. These P_h values are substituted for multiple linear regression model of the sensors having coefficients selected from Table 4.11. Then, the P_h expected at each sensor location is predicted.

If the measured P_h at any of the sensors location deviates significantly from the predicted one, it could be suggested that there is a problem in the dam in handling the reservoir water.

Using the procedure stated above a number of reservoir water levels was selected to compute the P_h expected at each of the sensors location and the final monitoring curve is shown below in Figure 4.8.

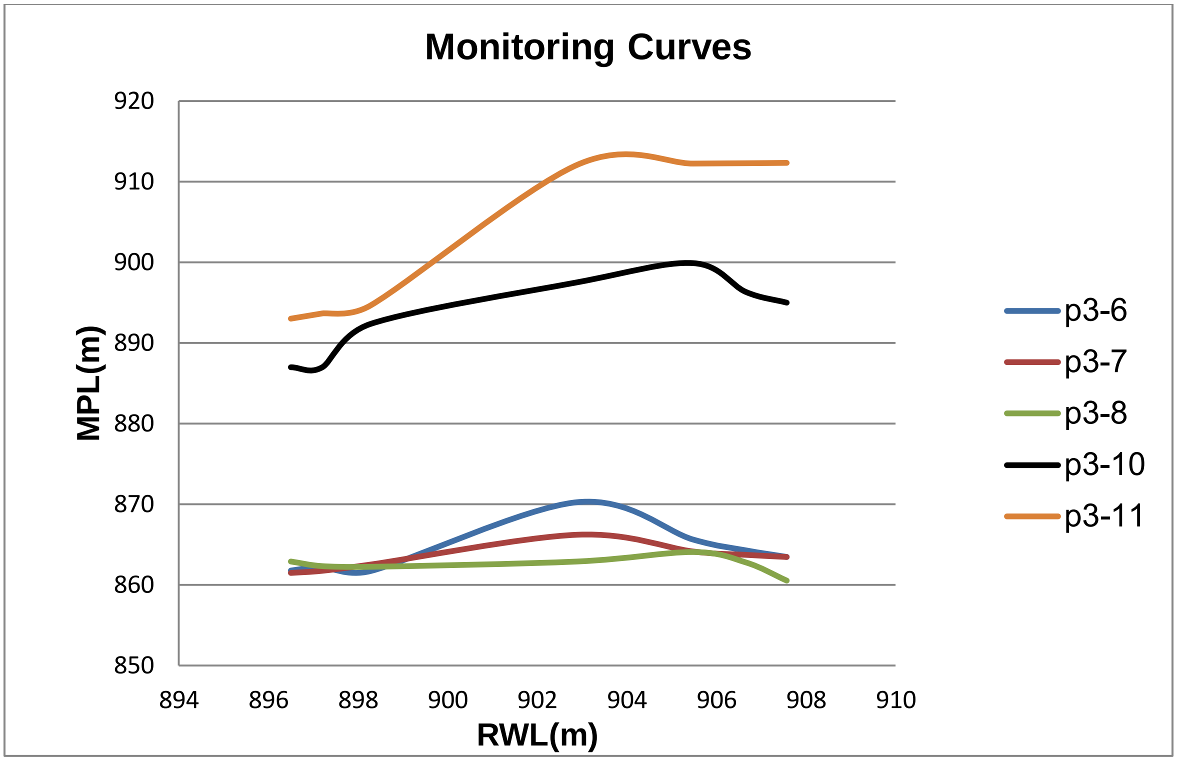

Figure 4.8 Monitoring Curves

5. CONCLUSION AND RECOMMENDATIONS

5.1 Conclusion

The methodology used in Kesem dam was to take core-samples at different location and time and measure the hydraulic conductivity of these samples in laboratory. The designed hydraulic conductivity is then compared with the laboratory one. Such approach do not represent the whole core of the dam and depends on the experience and choice of the expert on how to decide these sample locations.

In this study, construction quality monitoring of Kesem dam using pore water pressure was assessed with the help of SEEP/W model. Pore pressures measured at different locations in the core during construction are used for construction quality monitoring. The method at first predict the pore pressures at known locations (pore pressure sensor locations) for different values of the hydraulic conductivities for a given reservoir level. A number of hydraulic conductivities are used because any uniform hydraulic conductivity has seldom resulted in accurate pore pressure prediction. A number of pore pressure values are predicted using different hydraulic conductivity values.

The predicted pore pressures and the reservoir water level is then used as an input to a Multiple Linear Regression (MLR) analysis. MLR needs its coefficients to be determined. Thus, previously measured pore pressure data are used in MLR for its coefficients estimation.

Once MLR coefficients are estimated the construction quality is monitored on the basis of comparison of expected pore pressures obtained by the method described and the measured pore pressure values. If the comparison shows significant variation and sensors are working properly, then the construction quality is not as expected.

Five different hydraulic conductivity values were used ($6*10^{-6}$, $6*10^{-5}$,$6*10^{-4}$,$6*10^{-7}$, $6*10^{-8}$) and SEEP/W predicted the pore pressures at given sensor locations

(P_{3-6}, P_{3-7}, P_{3-8}, P_{3-10}, P_{3-11}) for reservoir water levels of 896.5, 897.20, 898.28, 902.89, 905.48, 906.66, 907.57. The result obtained by SEEP/W and the reservoir water level input a MLR analysis was done for regression coefficients estimation. The MLR coefficients obtained has R^2 value of nearly unity. By using these hydraulic conductivity and regression coefficients, monitoring curves drawn for any reservoir level in the dam. Existing dam safety monitoring techniques such as instrumentations (piezometric cells to to know pore pressure development, temperature measurements to get valuable information about seepage etc.) were investigated in this study.

5.2 Recommendations

Construction quality monitoring technique of Kesem dam using pore water pressure and seepage was done in this research, by using the relationship between the result from the model and the recorded values of the piezometric readings. The result of the pore water pressure in the piezometric areas from the model is almost the same as the result that was obtained from the recorded data. This result shows that the techniques of construction monitoring used is applicable and practicable if more representative piezometer values are used.

This modeling result gives not only the current condition of embankment dam construction monitoring, but also used to monitor the safety of the dam in the future by using reservoir water level as an input and comparing the predicted value with the measured one. Thus the future condition can be easily identified by checking the deviation between the measured piezometric head at any of the sensor location to the predicted value.

On some of the piezometric data the records are as few as a month data. Hence it is important to take piezometric records on each instrument stations.

In addition to this, the analysis will give better result when various points are taken at different elevation up to the reservoir normal supply level when it becomes full. That is in this research modeling was done at the early reservoir filling stage from reservoir water level 896.5m up to 907.57m. This will be better if subsequent modeling is done until steady state achieved after reservoir filling.

6. APPENDICES

6.1 Appendix to Chapter Four

6.1.1 SEEP/W Result at 896.5 WL

@896.5 when K=6*10-4

Node 1637, Steady-State value	P3-6	P3-7	P3-8	P3-9	P3-10	P3-11
X-Coordinate	243.88	260.93	274.3	253.08	269.52	260.92
Y-Coordinate	861.97	863.27	863.93	890.46	889.92	915.85
Z-Coordinate	0	0	0	0	0	0
Total Head	886.44	883.21	880.7	885.52	881.72	884.16
Pressure	239.97	195.52	164.47	-48.352	-80.434	-310.74
Pressure Head	24.469	19.937	16.771	-4.9304	-8.2017	-31.685
Boundary Flux	0	0	0	0	0	0
Cumulative Boundary Flux	0	0	0	0	0	0
X-Velocity	0.000122	0.000113	0.000113	0.000139	0.000138	0.000169
Y-Velocity	3.15E-05	1.26E-05	2.32E-06	1.64E-05	1.7E-06	1.46E-05
XY-Velocity	0.000126	0.000113	0.000113	0.00014	0.000138	0.000169
X-Gradient	0.2027	0.18789	0.18876	0.23187	0.22976	0.28142
Y-Gradient	0.052536	0.021393	0.003117	0.027338	0.002775	0.024648
XY-Gradient	0.2094	0.18911	0.18879	0.23348	0.22978	0.28249
X-Conductivity	0.0006	0.0006	0.0006	0.0006	0.0006	0.0006
Y-Conductivity	0.0006	0.0006	0.0006	0.0006	0.0006	0.0006
Vol. Water Content	0	0	0	0	0	0
Vol. W.C. Fn. Slope	0	0	0	0	0	0.00E+00

@896.5 when K=6*10-5

Node 1637, Steady-State value	P3-6	P3-7	P3-8	P3-9	P3-10	P3-11
X-Coordinate	243.88	260.93	274.3	253.08	253.08	260.92
Y-Coordinate	861.97	863.27	863.93	890.46	890.46	915.85
Z-Coordinate	0	0	0	0	0	0
Total Head	891.08	883.11	876.86	890.35	890.35	888.95
Pressure	285.5	194.53	126.82	-1.0189	-1.0189	-263.72
Pressure Head	29.111	19.836	12.931	-0.1039	-0.1039	-26.891
Boundary Flux	0	0	0	0	0	0
Cumulative Boundary Flux	0	0	0	0	0	0
X-Velocity	3.03E-05	2.8E-05	2.81E-05	3.94E-05	3.94E-05	6.74E-05
Y-Velocity	1E-05	4.01E-06	1.13E-06	9.94E-06	9.94E-06	1.58E-05
XY-Velocity	3.19E-05	2.83E-05	2.82E-05	4.06E-05	4.06E-05	6.92E-05
X-Gradient	0.50429	0.4675	0.46905	0.65637	0.65637	1.1248
Y-Gradient	0.16722	0.068571	0.028018	0.16609	0.16609	0.26566
XY-Gradient	0.53129	0.4725	0.46988	0.67706	0.67706	1.1557
X-Conductivity	0.00006	0.00006	0.00006	0.00006	0.00006	0.00006
Y-Conductivity	0.00006	0.00006	0.00006	0.00006	0.00006	0.00006
Vol. Water Content	0	0	0	0	0	0
Vol. W.C. Fn. Slope	0	0	0	0	0	0

@896.5 when K=6*10-6

Node 1637, Steady-State value	P3-6	P3-7	P3-8	P3-9	P3-10	P3-11
X-Coordinate	243.88	260.93	274.3	253.08	269.52	260.92
Y-Coordinate	861.97	863.27	863.93	890.46	889.92	915.85
Z-Coordinate	0	0	0	0	0	0
Total Head	893.64	882.73	874.49	893.41	877.46	892.37
Pressure	310.55	190.83	103.52	29.002	-122.2	-230.27
Pressure Head	31.666	19.459	10.556	2.9573	-12.46	-23.48
Boundary Flux	0	0	0	0	0	0
Cumulative Boundary Flux	0	0	0	0	0	0
X-Velocity	4.52E-06	3.71E-06	3.72E-06	5.55E-06	5.89E-06	1.02E-05
Y-Velocity	1.76E-06	6.98E-07	2.32E-07	1.59E-06	1.23E-07	2.66E-06
XY-Velocity	4.85E-06	3.77E-06	3.73E-06	5.77E-06	5.9E-06	1.05E-05
X-Gradient	0.7536	0.61845	0.62076	0.92542	0.9832	1.6973
Y-Gradient	0.2928	0.11957	0.051022	0.26522	0.00605	0.44793
XY-Gradient	0.80848	0.62991	0.62285	0.96268	0.98322	1.7554
X-Conductivity	0.000006	0.000006	0.000006	0.000006	0.000006	0.000006

Y-Conductivity	0.000006	0.000006	0.000006	0.000006	0.000006	0.000006
Vol. Water Content	0	0	0	0	0	0
Vol. W.C. Fn. Slope	0	0	0	0	0	0

@896.5 when K=6*10-7

Node 1637, Steady-State value	P3-6	P3-7	P3-8	P3-9	P3-10	P3-11
X-Coordinate	243.88	260.93	274.3	253.08	269.52	260.92
Y-Coordinate	861.97	863.27	863.93	890.46	889.92	915.85
Z-Coordinate	0	0	0	0	0	0
Total Head	893.94	882.52	874.09	893.92	877.17	892.94
Pressure	313.5	188.74	99.633	33.996	-124.99	-224.64
Pressure Head	31.967	19.245	10.159	3.4665	-12.745	-22.906
Boundary Flux	0	0	0	0	0	0
Cumulative Boundary Flux	0	0	0	0	0	0
X-Velocity	5.01E-07	3.79E-07	3.81E-07	5.83E-07	6.18E-07	1.07E-06
Y-Velocity	2.08E-07	8.15E-08	2.37E-08	1.69E-07	1.26E-08	2.84E-07
XY-Velocity	5.43E-07	3.88E-07	3.81E-07	6.07E-07	6.19E-07	1.11E-06
X-Gradient	0.83539	0.63343	0.63516	0.97156	1.0316	1.793
Y-Gradient	0.34716	0.13969	0.055939	0.28257	0.005696	0.47863
XY-Gradient	0.90465	0.64865	0.63762	1.0118	1.0317	1.8558
X-Conductivity	6E-07	6E-07	6E-07	6E-07	6E-07	6E-07
Y-Conductivity	6E-07	6E-07	6E-07	6E-07	6E-07	6E-07
Vol. Water Content	0	0	0	0	0	0
Vol. W.C. Fn. Slope	0	0	0	0	0	0

@896.5 when K=6*10-8

Node 1637, Steady-State value	P3-6	P3-7	P3-8	P3-9	P3-10	P3-11
X-Coordinate	243.88	260.93	274.3	253.08	269.52	260.92
Y-Coordinate	861.97	863.27	863.93	890.46	889.92	915.85
Z-Coordinate	0	0	0	0	0	0
Total Head	893.96	882.48	874.05	893.98	877.14	893
Pressure	313.71	188.37	99.189	34.537	-125.31	-224.03
Pressure Head	31.988	19.208	10.114	3.5217	-12.777	-22.844
Boundary Flux	0	0	0	0	0	0
Cumulative Boundary Flux	0	0	0	0	0	0
X-Velocity	5.09E-08	3.8E-08	3.81E-08	5.86E-08	6.22E-08	1.08E-07
Y-Velocity	2.13E-08	8.34E-09	2.34E-09	1.7E-08	1.26E-09	2.86E-08
XY-Velocity	5.51E-08	3.89E-08	3.82E-08	6.1E-08	6.22E-08	1.12E-07
X-Gradient	0.84789	0.63427	0.63586	0.97672	1.0369	1.8034
Y-Gradient	0.35609	0.14291	0.056441	0.28452	0.005561	0.48196
XY-Gradient	0.91963	0.65018	0.63836	1.0173	1.0369	1.8667

X-Conductivity	6E-08	6E-08	6E-08	6E-08	6E-08	6E-08
Y-Conductivity	6E-08	6E-08	6E-08	6E-08	6E-08	6E-08
Vol. Water Content	0	0	0	0	0	0
Vol. W.C. Fn. Slope	0	0	0	0	0	0

6.1.2 SEEP/W Result at 897.20 WL

@897.20 when K=6*10-4

Node 1637, Steady-State value	P3-6	P3-7	P3-8	P3-9	P3-10	P3-11
X-Coordinate	243.88	260.93	274.3	253.08	269.52	260.92
Y-Coordinate	861.97	863.27	863.93	890.46	889.92	915.85
Z-Coordinate	0	0	0	0	0	0
Total Head	887.27	883.95	881.37	886.33	882.41	884.93
Pressure	248.08	202.75	171.01	-40.453	-73.594	-303.2
Pressure Head	25.297	20.674	17.437	-4.1249	-7.5042	-30.917
Boundary Flux	0	0	0	0	0	0
Cumulative Boundary Flux	0	0	0	0	0	0
X-Velocity	0.000125	0.000116	0.000116	0.000143	0.000142	0.000174
Y-Velocity	3.25E-05	1.3E-05	2.34E-06	1.69E-05	1.79E-06	1.5E-05
XY-Velocity	0.000129	0.000117	0.000116	0.000144	0.000142	0.000174
X-Gradient	0.20844	0.19317	0.19404	0.23846	0.23627	0.28945
Y-Gradient	0.054136	0.02213	0.003105	0.02822	0.002921	0.025382
XY-Gradient	0.21536	0.19444	0.19406	0.24012	0.23628	0.29056
X-Conductivity	0.0006	0.0006	0.0006	0.0006	0.0006	0.0006
Y-Conductivity	0.0006	0.0006	0.0006	0.0006	0.0006	0.0006
Vol. Water Content	0	0	0	0	0	0
Vol. W.C. Fn. Slope	0	0	0	0	0	0

@897.20 when K=6*10-5

Node 1637, Steady-State value	P3-6	P3-7	P3-8	P3-9	P3-10	P3-11
X-Coordinate	243.88	260.93	274.3	253.08	269.52	260.92
Y-Coordinate	861.97	863.27	863.93	890.46	889.92	915.85
Z-Coordinate	0	0	0	0	0	0
Total Head	891.84	883.69	877.31	891.1	879.63	889.67
Pressure	292.98	200.23	131.15	6.3275	-100.94	-256.68
Pressure Head	29.874	20.417	13.373	0.6452	-10.292	-26.173
Boundary Flux	0	0	0	0	0	0
Cumulative Boundary Flux	0	0	0	0	0	0
X-Velocity	3.1E-05	2.87E-05	2.88E-05	4.03E-05	4.23E-05	6.89E-05
Y-Velocity	1.03E-05	4.12E-06	1.11E-06	1.02E-05	7.39E-07	1.61E-05
XY-Velocity	3.26E-05	2.9E-05	2.88E-05	4.15E-05	4.23E-05	7.08E-05
X-Gradient	0.51597	0.47805	0.4795	0.6712	0.70486	1.1501
Y-Gradient	0.17121	0.07041	0.028414	0.16991	0.003279	0.27166

XY-Gradient	0.54363	0.48321	0.48035	0.69237	0.70486	1.1818
X-Conductivity	0.00006	0.00006	0.00006	0.00006	0.00006	0.00006
Y-Conductivity	0.00006	0.00006	0.00006	0.00006	0.00006	0.00006
Vol. Water Content	0	0	0	0	0	0
Vol. W.C. Fn. Slope	0	0	0	0	0	0

@897.20 when K=6*10-6

Node 1637, Steady-State value	P3-6	P3-7	P3-8	P3-9	P3-10	P3-11
X-Coordinate	243.88	260.93	274.3	253.08	269.52	260.92
Y-Coordinate	861.97	863.27	863.93	890.46	889.92	915.85
Z-Coordinate	0	0	0	0	0	0
Total Head	894.32	883.21	874.81	894.09	877.84	893.03
Pressure	317.26	195.53	106.71	35.683	-118.45	-223.78
Pressure Head	32.351	19.938	10.881	3.6385	-12.078	-22.818
Boundary Flux	0	0	0	0	0	0
Cumulative Boundary Flux	0	0	0	0	0	0
X-Velocity	4.61E-06	3.78E-06	3.79E-06	5.66E-06	6E-06	1.04E-05
Y-Velocity	1.79E-06	7.12E-07	2.35E-07	1.62E-06	1.25E-07	2.71E-06
XY-Velocity	4.94E-06	3.84E-06	3.8E-06	5.88E-06	6.01E-06	1.07E-05
X-Gradient	0.76791	0.63005	0.63233	0.94277	1.0016	1.7291
Y-Gradient	0.29841	0.12195	0.051863	0.27021	0.006126	0.45632
XY-Gradient	0.82386	0.64174	0.63446	0.98073	1.0016	1.7883
X-Conductivity	0.000006	0.000006	0.000006	0.000006	0.000006	0.000006
Y-Conductivity	0.000006	0.000006	0.000006	0.000006	0.000006	0.000006
Vol. Water Content	0	0	0	0	0	0
Vol. W.C. Fn. Slope	0	0	0	0	0	0

@897.20 when K=6*10-7

Node 1637, Steady-State value	P3-6	P3-7	P3-8	P3-9	P3-10	P3-11
X-Coordinate	243.88	260.93	274.3	253.08	269.52	260.92
Y-Coordinate	861.97	863.27	863.93	890.46	889.92	915.85
Z-Coordinate	0	0	0	0	0	0
Total Head	894.6	882.98	874.4	894.59	877.54	893.59
Pressure	320.04	193.25	102.65	40.538	-121.42	-218.27
Pressure Head	32.634	19.705	10.467	4.1336	-12.381	-22.257
Boundary Flux	0	0	0	0	0	0
Cumulative Boundary Flux	0	0	0	0	0	0
X-Velocity	5.1E-07	3.86E-07	3.88E-07	5.93E-07	6.3E-07	1.09E-06
Y-Velocity	2.12E-07	8.3E-08	2.4E-08	1.72E-07	1.29E-08	2.89E-07
XY-Velocity	5.52E-07	3.95E-07	3.88E-07	6.18E-07	6.3E-07	1.13E-06
X-Gradient	0.85059	0.64488	0.64662	0.98913	1.0503	1.8255
Y-Gradient	0.35349	0.14228	0.0569	0.28769	0.005784	0.48728

XY-Gradient	0.92112	0.66039	0.64912	1.0301	1.0503	1.8894
X-Conductivity	6E-07	6E-07	6E-07	6E-07	6E-07	6E-07
Y-Conductivity	6E-07	6E-07	6E-07	6E-07	6E-07	6E-07
Vol. Water Content	0	0	0	0	0	0
Vol. W.C. Fn. Slope	0	0	0	0	0	0

@897.20 when K=6*10-8

Node 1637, Steady-State value	P3-6	P3-7	P3-8	P3-9	P3-10	P3-11
X-Coordinate	243.88	260.93	274.3	253.08	269.52	260.92
Y-Coordinate	861.97	863.27	863.93	890.46	889.92	915.85
Z-Coordinate	0	0	0	0	0	0
Total Head	894.62	882.94	874.35	894.64	877.5	893.65
Pressure	320.23	192.86	102.19	41.064	-121.75	-217.67
Pressure Head	32.653	19.666	10.42	4.1872	-12.415	-22.196
Boundary Flux	0	0	0	0	0	0
Cumulative Boundary Flux	0	0	0	0	0	0
X-Velocity	5.18E-08	3.87E-08	3.88E-08	5.96E-08	6.33E-08	1.1E-07
Y-Velocity	2.17E-08	8.49E-09	2.37E-09	1.73E-08	1.28E-09	2.91E-08
XY-Velocity	5.61E-08	3.96E-08	3.89E-08	6.21E-08	6.33E-08	1.14E-07
X-Gradient	0.86323	0.6457	0.64729	0.99431	1.0555	1.8359
Y-Gradient	0.36255	0.14554	0.057416	0.28966	0.005648	0.49064
XY-Gradient	0.93628	0.6619	0.64983	1.0356	1.0555	1.9003
X-Conductivity	6E-08	6E-08	6E-08	6E-08	6E-08	6E-08
Y-Conductivity	6E-08	6E-08	6E-08	6E-08	6E-08	6E-08
Vol. Water Content	0	0	0	0	0	0
Vol. W.C. Fn. Slope	0	0	0	0	0	0

6.1.3 SEEP/W Result at 898.28 WL

@898.28 when K=6*10-4

Node 1637, Steady-State value	P3-6	P3-7	P3-8	P3-9	P3-10	P3-11
X-Coordinate	243.88	260.93	274.3	253.08	269.52	260.92
Y-Coordinate	861.97	863.27	863.93	890.46	889.92	915.85
Z-Coordinate	0	0	0	0	0	0
Total Head	888.37	884.93	882.26	887.41	883.35	885.95
Pressure	258.93	212.4	179.74	-29.909	-64.463	-293.15
Pressure Head	26.402	21.658	18.328	-3.0498	-6.5732	-29.892
Boundary Flux	0	0	0	0	0	0
Cumulative Boundary Flux	0	0	0	0	0	0
X-Velocity	0.00013	0.00012	0.000121	0.000148	0.000147	0.00018
Y-Velocity	3.37E-05	1.36E-05	2.38E-06	1.76E-05	1.9E-06	1.56E-05
XY-Velocity	0.000134	0.000121	0.000121	0.000149	0.000147	0.000181
X-Gradient	0.21607	0.20022	0.20109	0.24724	0.24494	0.30015
Y-Gradient	0.056239	0.023077	0.003116	0.029382	0.003105	0.026356
XY-Gradient	0.22327	0.20154	0.20111	0.24898	0.24496	0.30131

X-Conductivity	0.0006	0.0006	0.0006	0.0006	0.0006	0.0006
Y-Conductivity	0.0006	0.0006	0.0006	0.0006	0.0006	0.0006
Vol. Water Content	0	0	0	0	0	0
Vol. W.C. Fn. Slope	0	0	0	0	0	0

@898.28 when K=6*10-5

Node 1637, Steady-State value	P3-6	P3-7	P3-8	P3-9	P3-10	P3-11
X-Coordinate	243.88	260.93	274.3	253.08	269.52	260.92
Y-Coordinate	861.97	863.27	863.93	890.46	889.92	915.85
Z-Coordinate	0	0	0	0	0	0
Total Head	892.93	884.52	877.94	892.17	880.33	890.7
Pressure	303.62	208.35	137.32	16.773	-94.017	-246.66
Pressure Head	30.96	21.245	14.002	1.7103	-9.5867	-25.151
Boundary Flux	0	0	0	0	0	0
Cumulative Boundary Flux	0	0	0	0	0	0
X-Velocity	3.19E-05	2.96E-05	2.97E-05	4.15E-05	4.36E-05	7.11E-05
Y-Velocity	1.06E-05	4.27E-06	1.08E-06	1.05E-05	7.56E-07	1.66E-05
XY-Velocity	3.37E-05	2.99E-05	2.97E-05	4.28E-05	4.36E-05	7.3E-05
X-Gradient	0.53241	0.49303	0.4944	0.69225	0.7269	1.1861
Y-Gradient	0.17679	0.072902	0.029074	0.17531	0.003295	0.28019
XY-Gradient	0.561	0.49839	0.49525	0.71411	0.7269	1.2188
X-Conductivity	0.00006	0.00006	0.00006	0.00006	0.00006	0.00006
Y-Conductivity	0.00006	0.00006	0.00006	0.00006	0.00006	0.00006
Vol. Water Content	0	0	0	0	0	0
Vol. W.C. Fn. Slope	0	0	0	0	0	0

@898.28 when K=6*10-6

Node 1637, Steady-State value	P3-6	P3-7	P3-8	P3-9	P3-10	P3-11
X-Coordinate	243.88	260.93	274.3	253.08	269.52	260.92
Y-Coordinate	861.97	863.27	863.93	890.46	889.92	915.85
Z-Coordinate	0	0	0	0	0	0
Total Head	895.36	883.94	875.31	895.12	878.42	894.03
Pressure	327.41	202.64	111.54	45.781	-112.78	-213.97
Pressure Head	33.386	20.663	11.373	4.6682	-11.5	-21.818
Boundary Flux	0	0	0	0	0	0
Cumulative Boundary Flux	0	0	0	0	0	0
X-Velocity	4.74E-06	3.88E-06	3.9E-06	5.81E-06	6.17E-06	1.07E-05
Y-Velocity	1.84E-06	7.33E-07	2.4E-07	1.66E-06	1.29E-07	2.78E-06
XY-Velocity	5.08E-06	3.95E-06	3.9E-06	6.05E-06	6.17E-06	1.1E-05
X-Gradient	0.78944	0.64757	0.64985	0.96898	1.0294	1.7771

Y-Gradient	0.30682	0.12547	0.053193	0.27774	0.006261	0.469
XY-Gradient	0.84696	0.65961	0.65203	1.008	1.0294	1.838
X-Conductivity	0.000006	0.000006	0.000006	0.000006	0.000006	0.000006
Y-Conductivity	0.000006	0.000006	0.000006	0.000006	0.000006	0.000006
Vol. Water Content	0	0	0	0	0	0
Vol. W.C. Fn. Slope	0	0	0	0	0	0

@898.28 when K=6*10-7

Node 1637, Steady-State value	P3-6	P3-7	P3-8	P3-9	P3-10	P3-11
X-Coordinate	243.88	260.93	274.3	253.08	269.52	260.92
Y-Coordinate	861.97	863.27	863.93	890.46	889.92	915.85
Z-Coordinate	0	0	0	0	0	0
Total Head	895.62	883.68	874.87	895.61	878.1	894.58
Pressure	330.06	200.16	107.28	50.555	-115.95	-208.52
Pressure Head	33.655	20.41	10.939	5.155	-11.823	-21.262
Boundary Flux	0	0	0	0	0	0
Cumulative Boundary Flux	0	0	0	0	0	0
X-Velocity	5.24E-07	3.97E-07	3.98E-07	6.1E-07	6.47E-07	1.12E-06
Y-Velocity	2.18E-07	8.53E-08	2.46E-08	1.77E-07	1.32E-08	2.97E-07
XY-Velocity	5.67E-07	4.06E-07	3.99E-07	6.35E-07	6.47E-07	1.16E-06
X-Gradient	0.8738	0.66242	0.66418	1.016	1.0788	1.8751
Y-Gradient	0.36316	0.1462	0.0584	0.29552	0.005926	0.50053
XY-Gradient	0.94626	0.67836	0.66674	1.0581	1.0788	1.9407
X-Conductivity	6E-07	6E-07	6E-07	6E-07	6E-07	6E-07
Y-Conductivity	6E-07	6E-07	6E-07	6E-07	6E-07	6E-07
Vol. Water Content	0	0	0	0	0	0
Vol. W.C. Fn. Slope	0	0	0	0	0	0

@898.28 when K=6*10-8

Node 1637, Steady-State value	P3-6	P3-7	P3-8	P3-9	P3-10	P3-11
X-Coordinate	243.88	260.93	274.3	253.08	269.52	260.92
Y-Coordinate	861.97	863.27	863.93	890.46	889.92	915.85
Z-Coordinate	0	0	0	0	0	0
Total Head	895.64	883.64	874.82	895.66	878.06	894.64
Pressure	330.23	199.75	106.8	51.072	-116.3	-207.93
Pressure Head	33.673	20.368	10.89	5.2077	-11.859	-21.202
Boundary Flux	0	0	0	0	0	0
Cumulative Boundary Flux	0	0	0	0	0	0
X-Velocity	5.32E-08	3.97E-08	3.99E-08	6.13E-08	6.5E-08	1.13E-07
Y-Velocity	2.23E-08	8.73E-09	2.43E-09	1.78E-08	1.31E-09	2.99E-08
XY-Velocity	5.77E-08	4.07E-08	3.99E-08	6.38E-08	6.5E-08	1.17E-07
X-Gradient	0.88672	0.66321	0.66482	1.0213	1.0841	1.8857
Y-Gradient	0.37243	0.14953	0.058935	0.29752	0.005789	0.50394
XY-Gradient	0.96175	0.67986	0.66743	1.0637	1.0842	1.9519

X-Conductivity	6E-08	6E-08	6E-08	6E-08	6E-08	6E-08
Y-Conductivity	6E-08	6E-08	6E-08	6E-08	6E-08	6E-08
Vol. Water Content	0	0	0	0	0	0
Vol. W.C. Fn. Slope	0	0	0	0	0	0

6.1.4 SEEP/W Result at 902.89 WL

@902.89 when K=6*10-4

Node 1637, Steady-State value	P3-6	P3-7	P3-8	P3-9	P3-10	P3-11
X-Coordinate	243.88	260.93	274.3	253.08	269.52	260.92
Y-Coordinate	861.97	863.27	863.93	890.46	889.92	915.85
Z-Coordinate	0	0	0	0	0	0
Total Head	893.13	889.17	886.1	892.04	887.36	890.38
Pressure	305.56	253.96	217.37	15.546	-25.094	-249.75
Pressure Head	31.157	25.896	22.165	1.5852	-2.5588	-25.466
Boundary Flux	0	0	0	0	0	0
Cumulative Boundary Flux	0	0	0	0	0	0
X-Velocity	0.000149	0.000138	0.000139	0.000171	0.000169	0.000208
Y-Velocity	3.92E-05	1.61E-05	2.49E-06	2.08E-05	2.45E-06	1.82E-05
XY-Velocity	0.000154	0.000139	0.000139	0.000172	0.000169	0.000209
X-Gradient	0.24854	0.23037	0.23134	0.28509	0.2823	0.34652
Y-Gradient	0.065441	0.027296	0.003057	0.034733	0.004061	0.030679
XY-Gradient	0.25701	0.23198	0.23136	0.28719	0.28233	0.34787
X-Conductivity	0.0006	0.0006	0.0006	0.0006	0.0006	0.0006
Y-Conductivity	0.0006	0.0006	0.0006	0.0006	0.0006	0.0006
Vol. Water Content	0	0	0	0	0	0
Vol. W.C. Fn. Slope	0	0	0	0	0	0

@902.89 when K=6*10-5

Node 1637, Steady-State value	P3-6	P3-7	P3-8	P3-9	P3-10	P3-11
X-Coordinate	243.88	260.93	274.3	253.08	269.52	260.92
Y-Coordinate	861.97	863.27	863.93	890.46	889.92	915.85
Z-Coordinate	0	0	0	0	0	0
Total Head	897.56	888.05	880.62	896.72	883.35	895.06
Pressure	349.05	243.02	163.66	61.393	-64.454	-203.84
Pressure Head	35.592	24.78	16.688	6.2601	-6.5722	-20.785
Boundary Flux	0	0	0	0	0	0
Cumulative Boundary Flux	0	0	0	0	0	0
X-Velocity	3.62E-05	3.34E-05	3.35E-05	4.69E-05	4.92E-05	8.03E-05
Y-Velocity	1.2E-05	4.9E-06	9.82E-07	1.19E-05	8.19E-07	1.88E-05
XY-Velocity	3.81E-05	3.38E-05	3.35E-05	4.84E-05	4.92E-05	8.25E-05
X-Gradient	0.60255	0.55692	0.55794	0.78219	0.82105	1.3401
Y-Gradient	0.20075	0.083674	0.031786	0.19856	0.003272	0.31668
XY-Gradient	0.63511	0.56317	0.55885	0.807	0.82105	1.377
X-Conductivity	0.00006	0.00006	0.00006	0.00006	0.00006	0.00006

Y-Conductivity	0.00006	0.00006	0.00006	0.00006	0.00006	0.00006
Vol. Water Content	0	0	0	0	0	0
Vol. W.C. Fn. Slope	0	0	0	0	0	0

@902.89 when K=6*10-6

Node 1637, Steady-State value	P3-6	P3-7	P3-8	P3-9	P3-10	P3-11
X-Coordinate	243.88	260.93	274.3	253.08	269.52	260.92
Y-Coordinate	861.97	863.27	863.93	890.46	889.92	915.85
Z-Coordinate	0	0	0	0	0	0
Total Head	899.77	887.03	877.41	899.51	880.88	898.3
Pressure	370.69	232.96	132.12	88.846	-88.601	-172.12
Pressure Head	37.799	23.755	13.472	9.0594	-9.0345	-17.551
Boundary Flux	0	0	0	0	0	0
Cumulative Boundary Flux	0	0	0	0	0	0
X-Velocity	5.29E-06	4.33E-06	4.34E-06	6.48E-06	6.88E-06	1.19E-05
Y-Velocity	2.06E-06	8.21E-07	2.61E-07	1.86E-06	1.42E-07	3.1E-06
XY-Velocity	5.67E-06	4.41E-06	4.35E-06	6.74E-06	6.88E-06	1.23E-05
X-Gradient	0.88122	0.72224	0.72454	1.0808	1.148	1.982
Y-Gradient	0.34274	0.14054	0.058837	0.30989	0.006813	0.52309
XY-Gradient	0.94552	0.73579	0.72693	1.1243	1.148	2.0498
X-Conductivity	0.000006	0.000006	0.000006	0.000006	0.000006	0.000006
Y-Conductivity	0.000006	0.000006	0.000006	0.000006	0.000006	0.000006
Vol. Water Content	0	0	0	0	0	0
Vol. W.C. Fn. Slope	0	0	0	0	0	0

@902.89 when K=6*10-7

Node 1637, Steady-State value	P3-6	P3-7	P3-8	P3-9	P3-10	P3-11
X-Coordinate	243.88	260.93	274.3	253.08	270.45	260.92
Y-Coordinate	861.97	863.27	863.93	890.46	865.01	915.85
Z-Coordinate	0	0	0	0	0	0
Total Head	899.98	886.69	876.89	899.97	879.72	898.83
Pressure	372.78	229.65	127.02	93.282	144.26	-166.92
Pressure Head	38.012	23.417	12.952	9.5118	14.71	-17.021
Boundary Flux	0	0	0	0	0	0
Cumulative Boundary Flux	0	0	0	0	0	0
X-Velocity	5.83E-07	4.42E-07	4.43E-07	6.78E-07	4.54E-07	1.25E-06
Y-Velocity	2.42E-07	9.51E-08	2.71E-08	1.97E-07	6.2E-09	3.3E-07
XY-Velocity	6.32E-07	4.52E-07	4.44E-07	7.06E-07	4.54E-07	1.29E-06
X-Gradient	0.97278	0.7372	0.73906	1.1307	0.75696	2.0867
Y-Gradient	0.4044	0.16295	0.064792	0.32892	0.003713	0.55703

XY-Gradient	1.0535	0.75499	0.7419	1.1776	0.75697	2.1598
X-Conductivity	6E-07	6E-07	6E-07	6E-07	6E-07	6E-07
Y-Conductivity	6E-07	6E-07	6E-07	6E-07	6E-07	6E-07
Vol. Water Content	0	0	0	0	0	0
Vol. W.C. Fn. Slope	0	0	0	0	0	0

@902.89 when K=6*10-8

Node 1637, Steady-State value	P3-6	P3-7	P3-8	P3-9	P3-10	P3-11
X-Coordinate	243.88	260.93	274.3	253.08	269.52	260.92
Y-Coordinate	861.97	863.27	863.93	890.46	889.92	915.85
Z-Coordinate	0	0	0	0	0	0
Total Head	899.99	886.64	876.83	900.02	880.43	898.88
Pressure	372.88	229.13	126.44	93.761	-93.055	-166.36
Pressure Head	38.022	23.364	12.893	9.5606	-9.4886	-16.963
Boundary Flux	0	0	0	0	0	0
Cumulative Boundary Flux	0	0	0	0	0	0
X-Velocity	5.92E-08	4.42E-08	4.43E-08	6.82E-08	7.23E-08	1.26E-07
Y-Velocity	2.48E-08	9.72E-09	2.67E-09	1.98E-08	1.46E-09	3.33E-08
XY-Velocity	6.42E-08	4.53E-08	4.44E-08	7.1E-08	7.23E-08	1.3E-07
X-Gradient	0.98686	0.73791	0.73962	1.1363	1.2062	2.098
Y-Gradient	0.41457	0.16657	0.065411	0.33106	0.006386	0.5607
XY-Gradient	1.0704	0.75647	0.74251	1.1836	1.2062	2.1717
X-Conductivity	6E-08	6E-08	6E-08	6E-08	6E-08	6E-08
Y-Conductivity	6E-08	6E-08	6E-08	6E-08	6E-08	6E-08
Vol. Water Content	0	0	0	0	0	0
Vol. W.C. Fn. Slope	0	0	0	0	0	0

6.1.5 SEEP/W Result at 905.48 WL

@905.48 when K=6*10-4

Node 1637, Steady-State value	P3-6	P3-7	P3-8	P3-9	P3-10	P3-11
X-Coordinate	243.88	260.93	274.3	253.08	269.52	260.92
Y-Coordinate	861.97	863.27	863.93	890.46	889.92	915.85
Z-Coordinate	0	0	0	0	0	0
Total Head	895.79	891.54	888.25	894.64	889.61	892.87
Pressure	331.64	277.24	238.46	41.046	-3.0058	-225.36
Pressure Head	33.817	28.269	24.315	4.1854	-0.3065	-22.979
Boundary Flux	0	0	0	0	0	0
Cumulative Boundary Flux	0	0	0	0	0	0
X-Velocity	0.00016	0.000148	0.000149	0.000184	0.000182	0.000224
Y-Velocity	4.24E-05	1.76E-05	2.5E-06	2.28E-05	2.79E-06	1.97E-05
XY-Velocity	0.000165	0.000149	0.000149	0.000185	0.000182	0.000224
X-Gradient	0.26639	0.24711	0.24819	0.3063	0.30324	0.37269
Y-Gradient	0.070689	0.029754	0.002949	0.038011	0.004729	0.033209

XY-Gradient	0.27561	0.2489	0.2482	0.30865	0.30328	0.37417
X-Conductivity	0.0006	0.0006	0.0006	0.0006	0.0006	0.0006
Y-Conductivity	0.0006	0.0006	0.0006	0.0006	0.0006	0.0006
Vol. Water Content	0	0	0	0	0	0
Vol. W.C. Fn. Slope	0	0	0	0	0	0

@905.48 when K=6*10-5

Node 1637, Steady-State value	P3-6	P3-7	P3-8	P3-9	P3-10	P3-11
X-Coordinate	243.88	260.93	274.3	253.08	269.52	260.92
Y-Coordinate	861.97	863.27	863.93	890.46	889.92	915.85
Z-Coordinate	0	0	0	0	0	0
Total Head	900.15	890.03	882.12	899.26	885.03	897.5
Pressure	374.41	262.37	178.38	86.339	-47.926	-179.88
Pressure Head	38.178	26.754	18.189	8.8038	-4.8869	-18.342
Boundary Flux	0	0	0	0	0	0
Cumulative Boundary Flux	0	0	0	0	0	0
X-Velocity	3.85E-05	3.55E-05	3.56E-05	4.99E-05	5.24E-05	8.55E-05
Y-Velocity	1.28E-05	5.26E-06	1.25E-06	1.27E-05	8.49E-07	2E-05
XY-Velocity	4.06E-05	3.59E-05	3.56E-05	5.15E-05	5.24E-05	8.78E-05
X-Gradient	0.64161	0.59257	0.59341	0.83248	0.87368	1.4263
Y-Gradient	0.21419	0.089753	0.033256	0.2117	0.003196	0.33716
XY-Gradient	0.67642	0.59933	0.59434	0.85897	0.87368	1.4656
X-Conductivity	0.00006	0.00006	0.00006	0.00006	0.00006	0.00006
Y-Conductivity	0.00006	0.00006	0.00006	0.00006	0.00006	0.00006
Vol. Water Content	0	0	0	0	0	0
Vol. W.C. Fn. Slope	0	0	0	0	0	0

@905.48 when K=6*10-6

Node 1637, Steady-State value	P3-6	P3-7	P3-8	P3-9	P3-10	P3-11
X-Coordinate	243.88	260.93	274.3	253.08	269.52	260.92
Y-Coordinate	861.97	863.27	863.93	890.46	889.92	915.85
Z-Coordinate	0	0	0	0	0	0
Total Head	902.24	888.76	878.58	901.98	882.27	900.69
Pressure	394.95	249.96	143.66	112.99	-75.047	-148.66
Pressure Head	40.272	25.488	14.648	11.521	-7.6524	-15.159
Boundary Flux	0	0	0	0	0	0
Cumulative Boundary Flux	0	0	0	0	0	0
X-Velocity	5.59E-06	4.58E-06	4.59E-06	6.86E-06	7.28E-06	1.26E-05
Y-Velocity	2.18E-06	8.7E-07	2.73E-07	1.96E-06	1.5E-07	3.28E-06
XY-Velocity	6E-06	4.66E-06	4.6E-06	7.13E-06	7.28E-06	1.3E-05
X-Gradient	0.93264	0.7641	0.7664	1.1434	1.2145	2.0968

Y-Gradient	0.36287	0.14899	0.061996	0.32794	0.007112	0.55342
XY-Gradient	1.0007	0.77849	0.76891	1.1895	1.2145	2.1686
X-Conductivity	0.000006	0.000006	0.000006	0.000006	0.000006	0.000006
Y-Conductivity	0.000006	0.000006	0.000006	0.000006	0.000006	0.000006
Vol. Water Content	0	0	0	0	0	0
Vol. W.C. Fn. Slope	0	0	0	0	0	0

@905.48 when K=6*10-7

Node 1637, Steady-State value	P3-6	P3-7	P3-8	P3-9	P3-10	P3-11
X-Coordinate	243.88	260.93	274.3	260.92	269.52	260.92
Y-Coordinate	861.97	863.27	863.93	915.85	889.92	915.85
Z-Coordinate	0	0	0	0	0	0
Total Head	902.43	888.38	878.01	901.21	881.81	901.21
Pressure	396.76	246.19	138.1	-143.58	-79.513	-143.58
Pressure Head	40.456	25.104	14.082	-14.64	-8.1078	-14.64
Boundary Flux	0	0	0	0	0	0
Cumulative Boundary Flux	0	0	0	0	0	0
X-Velocity	6.17E-07	4.67E-07	4.68E-07	1.32E-06	7.61E-07	1.32E-06
Y-Velocity	2.56E-07	1.01E-07	2.84E-08	3.49E-07	1.54E-08	3.49E-07
XY-Velocity	6.68E-07	4.78E-07	4.69E-07	1.37E-06	7.61E-07	1.37E-06
X-Gradient	1.0283	0.77916	0.78108	2.2055	1.2689	2.2055
Y-Gradient	0.42754	0.17235	0.068382	0.58874	0.006862	0.58874
XY-Gradient	1.1136	0.79799	0.78407	2.2827	1.2689	2.2827
X-Conductivity	6E-07	6E-07	6E-07	6E-07	6E-07	6E-07
Y-Conductivity	6E-07	6E-07	6E-07	6E-07	6E-07	6E-07
Vol. Water Content	0	0	0	0	0	0
Vol. W.C. Fn. Slope	0	0	0	0	0	0

@905.48 when K=6*10-8

Node 1637, Steady-State value	P3-6	P3-7	P3-8	P3-9	P3-10	P3-11
X-Coordinate	243.88	260.93	274.3	253.08	269.52	260.92
Y-Coordinate	861.97	863.27	863.93	890.46	889.92	915.85
Z-Coordinate	0	0	0	0	0	0
Total Head	902.43	888.32	877.95	902.46	881.76	901.26
Pressure	396.82	245.62	137.47	117.72	-80.007	-143.03
Pressure Head	40.463	25.045	14.018	12.004	-8.1582	-14.584
Boundary Flux	0	0	0	0	0	0
Cumulative Boundary Flux	0	0	0	0	0	0
X-Velocity	6.26E-08	4.67E-08	4.69E-08	7.2E-08	7.64E-08	1.33E-07
Y-Velocity	2.63E-08	1.03E-08	2.81E-09	2.09E-08	1.54E-09	3.52E-08

XY-Velocity	6.78E-08	4.78E-08	4.69E-08	7.5E-08	7.64E-08	1.37E-07
X-Gradient	1.043	0.77983	0.7816	1.2009	1.2747	2.2172
Y-Gradient	0.43822	0.17613	0.06905	0.34989	0.006721	0.59255
XY-Gradient	1.1314	0.79947	0.78465	1.2508	1.2747	2.295
X-Conductivity	6E-08	6E-08	6E-08	6E-08	6E-08	6E-08
Y-Conductivity	6E-08	6E-08	6E-08	6E-08	6E-08	6E-08
Vol. Water Content	0	0	0	0	0	0
Vol. W.C. Fn. Slope	0	0	0	0	0	0

6.1.6 SEEP/W Result at 906.66 WL

@906.66 when K=6*10-4

Node 1637, Steady-State value	P3-6	P3-7	P3-8	P3-9	P3-10	P3-11
X-Coordinate	243.88	260.93	274.3	253.08	269.52	260.92
Y-Coordinate	861.97	863.27	863.93	890.46	889.92	915.85
Z-Coordinate	0	0	0	0	0	0
Total Head	897.05	892.68	889.28	895.89	890.69	894.06
Pressure	344.07	288.35	248.53	53.251	7.5671	-213.66
Pressure Head	35.084	29.403	25.342	5.4299	0.7716	-21.787
Boundary Flux	0	0	0	0	0	0
Cumulative Boundary Flux	0	0	0	0	0	0
X-Velocity	0.000165	0.000153	0.000154	0.00019	0.000188	0.000231
Y-Velocity	4.39E-05	1.83E-05	2.46E-06	2.38E-05	2.98E-06	2.04E-05
XY-Velocity	0.000171	0.000154	0.000154	0.000191	0.000188	0.000232
X-Gradient	0.27476	0.25504	0.25618	0.31644	0.31325	0.38532
Y-Gradient	0.073258	0.030994	0.002846	0.039737	0.005127	0.034479
XY-Gradient	0.28436	0.25691	0.2562	0.31892	0.31329	0.38686
X-Conductivity	0.0006	0.0006	0.0006	0.0006	0.0006	0.0006
Y-Conductivity	0.0006	0.0006	0.0006	0.0006	0.0006	0.0006
Vol. Water Content	0	0	0	0	0	0
Vol. W.C. Fn. Slope	0	0	0	0	0	0

@906.66 when K=6*10-5

Node 1637, Steady-State value	P3-6	P3-7	P3-8	P3-9	P3-10	P3-11
X-Coordinate	243.88	260.93	274.3	253.08	269.52	260.92
Y-Coordinate	861.97	863.27	863.93	890.46	889.92	915.85
Z-Coordinate	0	0	0	0	0	0
Total Head	901.35	890.94	882.82	900.44	885.82	898.64
Pressure	386.2	271.38	185.22	97.967	-40.223	-168.7
Pressure Head	39.38	27.672	18.887	9.9895	-4.1015	-17.202
Boundary Flux	0	0	0	0	0	0
Cumulative Boundary Flux	0	0	0	0	0	0
X-Velocity	3.96E-05	3.65E-05	3.66E-05	5.13E-05	5.39E-05	8.79E-05

Y-Velocity	1.32E-05	5.43E-06	1.34E-06	1.3E-05	8.58E-07	2.06E-05
XY-Velocity	4.17E-05	3.69E-05	3.66E-05	5.3E-05	5.39E-05	9.03E-05
X-Gradient	0.65981	0.60916	0.6099	0.85592	0.89821	1.4666
Y-Gradient	0.22052	0.092665	0.033878	0.21791	0.003113	0.34674
XY-Gradient	0.69568	0.61616	0.61084	0.88323	0.89822	1.507
X-Conductivity	0.00006	0.00006	0.00006	0.00006	0.00006	0.00006
Y-Conductivity	0.00006	0.00006	0.00006	0.00006	0.00006	0.00006
Vol. Water Content	0	0	0	0	0	0
Vol. W.C. Fn. Slope	0	0	0	0	0	0

@906.66 when K=6*10-6

Node 1637, Steady-State value	P3-6	P3-7	P3-8	P3-9	P3-10	P3-11
X-Coordinate	243.88	260.93	274.3	253.08	269.52	260.92
Y-Coordinate	861.97	863.27	863.93	890.46	889.92	915.85
Z-Coordinate	0	0	0	0	0	0
Total Head	903.37	889.55	879.12	903.1	882.9	901.78
Pressure	406.04	257.73	148.93	124.04	-68.846	-137.92
Pressure Head	41.403	26.28	15.186	12.648	-7.0201	-14.064
Boundary Flux	0	0	0	0	0	0
Cumulative Boundary Flux	0	0	0	0	0	0
X-Velocity	5.74E-06	4.69E-06	4.71E-06	7.03E-06	7.46E-06	1.29E-05
Y-Velocity	2.23E-06	8.93E-07	2.78E-07	2.01E-06	1.53E-07	3.37E-06
XY-Velocity	6.15E-06	4.78E-06	4.72E-06	7.31E-06	7.47E-06	1.33E-05
X-Gradient	0.95619	0.78325	0.78555	1.1721	1.2449	2.1494
Y-Gradient	0.37212	0.15289	0.063416	0.33622	0.007236	0.56731
XY-Gradient	1.026	0.79803	0.78811	1.2194	1.245	2.223
X-Conductivity	0.000006	0.000006	0.000006	0.000006	0.000006	0.000006
Y-Conductivity	0.000006	0.000006	0.000006	0.000006	0.000006	0.000006
Vol. Water Content	0	0	0	0	0	0
Vol. W.C. Fn. Slope	0	0	0	0	0	0

@906.66 when K=6*10-7

Node 1637, Steady-State value	P3-6	P3-7	P3-8	P3-9	P3-10	P3-11
X-Coordinate	243.88	260.93	274.3	253.08	269.52	260.92
Y-Coordinate	861.97	863.27	863.93	890.46	889.92	915.85
Z-Coordinate	0	0	0	0	0	0
Total Head	903.54	889.15	878.53	903.53	882.42	902.29
Pressure	407.69	253.74	143.15	128.2	-73.54	-132.93
Pressure Head	41.571	25.873	14.597	13.072	-7.4987	-13.555
Boundary Flux	0	0	0	0	0	0
Cumulative Boundary Flux	0	0	0	0	0	0
X-Velocity	6.32E-07	4.78E-07	4.8E-07	7.35E-07	7.79E-07	1.35E-06
Y-Velocity	2.63E-07	1.03E-07	2.91E-08	2.13E-07	1.58E-08	3.58E-07

XY-Velocity	6.84E-07	4.89E-07	4.81E-07	7.65E-07	7.8E-07	1.4E-06
X-Gradient	1.0536	0.7983	0.80025	1.2245	1.3001	2.2597
Y-Gradient	0.4381	0.17664	0.070011	0.35623	0.007011	0.60321
XY-Gradient	1.1411	0.81761	0.8033	1.2752	1.3001	2.3388
X-Conductivity	6E-07	6E-07	6E-07	6E-07	6E-07	6E-07
Y-Conductivity	6E-07	6E-07	6E-07	6E-07	6E-07	6E-07
Vol. Water Content	0	0	0	0	0	0
Vol. W.C. Fn. Slope	0	0	0	0	0	0

@906.66 when K=6*10-8

Node 1637, Steady-State value	P3-6	P3-7	P3-8	P3-9	P3-10	P3-11
X-Coordinate	243.88	260.93	274.3	253.08	269.52	260.92
Y-Coordinate	861.97	863.27	863.93	890.46	889.92	915.85
Z-Coordinate	0	0	0	0	0	0
Total Head	903.55	889.08	878.46	903.57	882.37	902.35
Pressure	407.73	253.14	142.5	128.64	-74.059	-132.39
Pressure Head	41.576	25.812	14.53	13.118	-7.5516	-13.5
Boundary Flux	0	0	0	0	0	0
Cumulative Boundary Flux	0	0	0	0	0	0
X-Velocity	6.41E-08	4.79E-08	4.8E-08	7.38E-08	7.83E-08	1.36E-07
Y-Velocity	2.69E-08	1.05E-08	2.87E-09	2.15E-08	1.58E-09	3.6E-08
XY-Velocity	6.95E-08	4.9E-08	4.81E-08	7.69E-08	7.83E-08	1.41E-07
X-Gradient	1.0687	0.79894	0.80074	1.2303	1.306	2.2715
Y-Gradient	0.44901	0.18049	0.070703	0.35848	0.006871	0.60708
XY-Gradient	1.1592	0.81907	0.80385	1.2815	1.306	2.3513
X-Conductivity	6E-08	6E-08	6E-08	6E-08	6E-08	6E-08
Y-Conductivity	6E-08	6E-08	6E-08	6E-08	6E-08	6E-08
Vol. Water Content	0	0	0	0	0	0
Vol. W.C. Fn. Slope	0	0	0	0	0	0

6.1.7 SEEP/W Result at 907.57 WL

@907.57 when K=6*10-4

Node 1637, Steady-State value	P3-6	P3-7	P3-8	P3-9	P3-10	P3-11
X-Coordinate	243.88	260.93	274.3	253.08	269.52	260.92
Y-Coordinate	861.97	863.27	863.93	890.46	889.92	915.85
Z-Coordinate	0	0	0	0	0	0
Total Head	898.11	893.62	890.14	896.93	891.59	895.06
Pressure	354.44	297.64	256.96	63.475	16.425	-203.84
Pressure Head	36.141	30.349	26.202	6.4724	1.6748	-20.785
Boundary Flux	0	0	0	0	0	0
Cumulative Boundary Flux	0	0	0	0	0	0
X-Velocity	0.000169	0.000157	0.000158	0.000195	0.000193	0.000238

Y-Velocity	4.53E-05	1.9E-05	2.39E-06	2.48E-05	3.17E-06	2.11E-05
XY-Velocity	0.000175	0.000158	0.000158	0.000197	0.000193	0.000239
X-Gradient	0.28158	0.26156	0.2628	0.32492	0.32162	0.39601
Y-Gradient	0.075475	0.032107	0.0027	0.041364	0.005549	0.035614
XY-Gradient	0.29151	0.26353	0.26281	0.32755	0.32166	0.39761
X-Conductivity	0.0006	0.0006	0.0006	0.0006	0.0006	0.0006
Y-Conductivity	0.0006	0.0006	0.0006	0.0006	0.0006	0.0006
Vol. Water Content	0	0	0	0	0	0
Vol. W.C. Fn. Slope	0	0	0	0	0	0

@907.57 when K=6*10-5

Node 1637, Steady-State value	P3-6	P3-7	P3-8	P3-9	P3-10	P3-11
X-Coordinate	243.88	260.93	274.3	253.08	269.52	260.92
Y-Coordinate	861.97	863.27	863.93	890.46	889.92	915.85
Z-Coordinate	0	0	0	0	0	0
Total Head	902.31	891.68	883.38	901.4	886.45	899.56
Pressure	395.65	278.59	190.7	107.31	-34.039	-159.7
Pressure Head	40.343	28.407	19.446	10.942	-3.4709	-16.285
Boundary Flux	0	0	0	0	0	0
Cumulative Boundary Flux	0	0	0	0	0	0
X-Velocity	4.05E-05	3.73E-05	3.74E-05	5.25E-05	5.5E-05	8.99E-05
Y-Velocity	1.35E-05	5.58E-06	1.42E-06	1.34E-05	8.6E-07	2.1E-05
XY-Velocity	4.27E-05	3.77E-05	3.74E-05	5.42E-05	5.5E-05	9.23E-05
X-Gradient	0.67441	0.62245	0.62309	0.87478	0.91793	1.499
Y-Gradient	0.22568	0.095105	0.034297	0.223	0.002988	0.35449
XY-Gradient	0.71117	0.62967	0.62403	0.90275	0.91793	1.5404
X-Conductivity	0.00006	0.00006	0.00006	0.00006	0.00006	0.00006
Y-Conductivity	0.00006	0.00006	0.00006	0.00006	0.00006	0.00006
Vol. Water Content	0	0	0	0	0	0
Vol. W.C. Fn. Slope	0	0	0	0	0	0

@907.57 when K=6*10-6

Node 1637, Steady-State value	P3-6	P3-7	P3-8	P3-9	P3-10	P3-11
X-Coordinate	243.88	260.93	274.3	253.08	269.52	260.92
Y-Coordinate	861.97	863.27	863.93	890.46	889.92	915.85
Z-Coordinate	0	0	0	0	0	0
Total Head	904.25	890.17	879.54	903.98	883.39	902.63
Pressure	414.66	263.76	153.02	132.63	-64.024	-129.57
Pressure Head	42.282	26.895	15.604	13.524	-6.5284	-13.212
Boundary Flux	0	0	0	0	0	0
Cumulative Boundary Flux	0	0	0	0	0	0
X-Velocity	5.85E-06	4.78E-06	4.8E-06	7.17E-06	7.61E-06	1.31E-05

Y-Velocity	2.27E-06	9.11E-07	2.81E-07	2.05E-06	1.56E-07	3.43E-06
XY-Velocity	6.27E-06	4.87E-06	4.81E-06	7.45E-06	7.61E-06	1.36E-05
X-Gradient	0.97455	0.79814	0.80042	1.1944	1.2686	2.1903
Y-Gradient	0.37934	0.15597	0.064486	0.34268	0.007316	0.57812
XY-Gradient	1.0458	0.81323	0.80302	1.2426	1.2686	2.2653
X-Conductivity	0.000006	0.000006	0.000006	0.000006	0.000006	0.000006
Y-Conductivity	0.000006	0.000006	0.000006	0.000006	0.000006	0.000006
Vol. Water Content	0	0	0	0	0	0
Vol. W.C. Fn. Slope	0	0	0	0	0	0

@907.57 when K=6*10-7

Node 1637, Steady-State value	P3-6	P3-7	P3-8	P3-9	P3-10	P3-11
X-Coordinate	243.88	260.93	274.3	253.08	269.52	260.92
Y-Coordinate	861.97	863.27	863.93	890.46	889.92	915.85
Z-Coordinate	0	0	0	0	0	0
Total Head	904.4	889.74	878.93	904.39	882.89	903.13
Pressure	416.14	259.57	147.05	136.65	-68.922	-124.7
Pressure Head	42.433	26.468	14.995	13.934	-7.0278	-12.715
Boundary Flux	0	0	0	0	0	0
Cumulative Boundary Flux	0	0	0	0	0	0
X-Velocity	6.44E-07	4.87E-07	4.89E-07	7.48E-07	7.94E-07	1.38E-06
Y-Velocity	2.67E-07	1.05E-07	2.95E-08	2.17E-07	1.61E-08	3.64E-07
XY-Velocity	6.97E-07	4.98E-07	4.89E-07	7.79E-07	7.94E-07	1.43E-06
X-Gradient	1.0733	0.8131	0.81506	1.2472	1.3242	2.3015
Y-Gradient	0.44628	0.17998	0.071259	0.36286	0.007121	0.6144
XY-Gradient	1.1623	0.83278	0.81817	1.2989	1.3242	2.3821
X-Conductivity	6E-07	6E-07	6E-07	6E-07	6E-07	6E-07
Y-Conductivity	6E-07	6E-07	6E-07	6E-07	6E-07	6E-07
Vol. Water Content	0	0	0	0	0	0
Vol. W.C. Fn. Slope	0	0	0	0	0	0

@907.57 when K=6*10-8

Node 1637, Steady-State value	P3-6	P3-7	P3-8	P3-9	P3-10	P3-11
X-Coordinate	243.88	260.93	274.3	253.08	269.52	260.92
Y-Coordinate	861.97	863.27	863.93	890.46	889.92	915.85
Z-Coordinate	0	0	0	0	0	0
Total Head	904.4	889.68	878.86	904.43	882.84	903.18
Pressure	416.16	258.94	146.38	137.08	-69.463	-124.17
Pressure Head	42.435	26.404	14.926	13.978	-7.083	-12.661
Boundary Flux	0	0	0	0	0	0
Cumulative Boundary Flux	0	0	0	0	0	0
X-Velocity	6.53E-08	4.87E-08	4.89E-08	7.52E-08	7.97E-08	1.39E-07

Y-Velocity	2.74E-08	1.07E-08	2.92E-09	2.19E-08	1.6E-09	3.67E-08
XY-Velocity	7.08E-08	4.99E-08	4.9E-08	7.83E-08	7.98E-08	1.43E-07
X-Gradient	1.0885	0.8137	0.81552	1.2531	1.3301	2.3135
Y-Gradient	0.45735	0.18388	0.071971	0.36512	0.006982	0.6183
XY-Gradient	1.1807	0.83422	0.81869	1.3052	1.3301	2.3947
X-Conductivity	6E-08	6E-08	6E-08	6E-08	6E-08	6E-08
Y-Conductivity	6E-08	6E-08	6E-08	6E-08	6E-08	6E-08
Vol. Water Content	0	0	0	0	0	0
Vol. W.C. Fn. Slope	0	0	0	0	0	0

Multiple Linear Regression input Data

pizometric ID	measured	K=10^-6	K=10^-4	K=10^-5	K=10^-7	K=10^-8	Wl
P3-6	861.76	893.64	886.44	891.08	893.94	893.96	896.5
	862.23	894.32	887.27	891.84	894.6	894.62	897.2
	861.71	895.36	888.37	892.93	895.62	895.64	898.28
	870.24	899.77	893.13	897.56	899.98	899.99	902.89
	865.61	902.24	895.79	900.15	902.43	902.43	905.48
	864.27	903.37	897.05	901.35	903.54	903.55	906.66
	863.46	904.25	898.11	902.31	904.4	904.4	907.57
P3-7	861.47	882.73	883.21	883.11	882.52	882.48	896.5
	861.74	883.21	883.94	883.69	882.98	882.94	897.2
	862.51	883.94	884.93	884.52	883.68	883.64	898.28
	866.21	887.03	889.17	888.05	886.69	886.64	902.89
	864.13	888.76	891.54	890.03	888.38	888.32	905.48
	863.71	889.55	892.68	890.94	889.15	889.08	906.66
	863.45	890.17	893.62	891.68	889.74	889.68	907.57
P3-8	862.89	874.49	880.7	876.86	874.09	874.05	896.5
	862.32	874.81	881.37	877.31	874.4	874.35	897.2
	862.23	875.31	882.26	877.94	874.87	874.82	898.28
	1383.00	877.41	886.1	880.62	876.89	876.83	902.89
	864.07	878.58	888.25	882.12	878.01	877.95	905.48
	862.77	879.12	889.28	882.82	878.53	878.46	906.66
	1642.86	879.54	890.14	883.38	878.93	878.86	907.57
P3-9	862.89	874.49	880.7	876.86	874.09	874.05	896.5
	862.32	874.81	881.37	877.31	874.4	874.35	897.2
	862.23	875.31	882.26	877.94	874.87	874.82	898.28
	1383.00	877.41	886.1	880.62	876.89	876.83	902.89
	864.07	878.58	888.25	882.12	878.01	877.95	905.48
	862.77	879.12	889.28	882.82	878.53	878.46	906.66
	1642.86	879.54	890.14	883.38	878.93	878.86	907.57
P3-10	886.98	877.46	881.72	879.13	877.17	877.14	896.5
	886.97	877.84	882.41	879.63	877.54	877.5	897.2
	892.35	878.42	883.35	880.33	878.1	878.06	898.28
	897.51	880.88	887.36	883.35	879.92	880.43	902.89
	899.89	882.27	889.61	885.03	881.81	881.76	905.48
	896.31	882.9	890.69	885.82	882.42	882.37	906.66
	894.99	883.39	891.59	886.45	882.89	882.84	907.57
P3-11	893.01	892.37	884.16	888.95	892.94	893	896.5
	893.65	893.03	884.93	889.67	893.59	893.65	897.2
	894.65	894.03	885.95	890.7	894.58	894.64	898.28
	912.08	898.3	890.38	895.06	898.83	898.88	902.89
	912.24	900.69	892.87	897.5	901.21	901.26	905.48
	912.28	901.78	894.06	898.64	902.29	902.35	906.66
	912.33	902.63	895.06	899.56	903.13	903.18	907.57

7. REFERENCES

1. Water Resources Policy (2008). "Guide Lines for the Construction of Earth fill dam." Tasmania.
2. USACE (1994). "Earth and Rock-Fill Dams-General Design and Construction Considerations." Engineer manual, United States.
3. USACE (1995). "Construction Control for Earth and Rock-Fill Dams." Engineer manual, United States.
4. G.Rakhshandehroo and A. Bagherieh (2006). "Three Dimensional Analysis of Seepage in 15-Khordad Dam After Impoundment." Journal of Science & Technology, Transaction B, Engineering, Vol. 30, No. B1. Shiraz, I. R. of Iran.
5. Dunnicliff, J. & Green, G. E. (1988). "Geotechnical instrumentation for monitoring field performance " John Wiley & Sons Publications.
6. USACE, (1995). "Instrumentation of embankment dams and levees." Engineer Manual, No. EM 1110-2-1908.
7. Kutzner, C. (1997). "Earth and Rock fill Dams principles of design and construction " Balkema.
8. Mebruk Mohammed, Kunio Watanabe, Shinji Takeuchi (2010). "Grey model for prediction of pore pressure change." Journal of Environ Earth Sci. Saitama338-8570, Japan.
9. Mr. Yuefei Zhou, Ms. Huanying Zeng,Ms. Fang Han and Mr. Yukun Wu,(2008). "Kesem Main Dam optimization report." Mid-South Design & Research Institute, CHECC, China.
10. Serafi, J. L., Santos, A. P. & Matos, M. C. (1985). "Three dimensional seepage through a dam foundation." Proceedings of 14th ICOLD, Lausanne, 767-779.
11. Shi, W., Y. Zheng and B. Tang, 2003. "Discussion on stability analysis method for landslides." Rock and Soil Mechanics-Wuhan, 24(4); ISSU 85: 545-548.
12. Zhou huifen,(2007) "Kesem Main Dam Fill Construction Technical Instruction" Mid-South Design & Research Institute, CHECC, China.
13. Jon Krah (2004), "Seepage Modeling with SEEP/W," Calgary, Alberta, Canada T2P2Y5

14. ICSE6 (2012) Pontus SJÖDAHL, Sam JOHANSSON. "Experiences from internal erosion detection and seepage monitoring based on temperature measurements on Swedish embankment dams." *ICSE6, Paris.*
15. Anna Szostak-Chrzanowski, Michel Massiéra, Adam Chrzanowski, Christopher J. Hill. "Use of geodetic monitoring surveys in verifying design parameters of large earthen dams at the stage of filling the reservoir." Canada.
16. Pingyu Zhua,Y.B. Lengb, Y.Zhoua,b and G.L. Jiang (2010). "Safety Inspection Strategy for Earth Embankment Dams using Fully Distributed Sensing." China.
17. Henry H.Thomas (1976), Hobart, "The engineering of Large Dams Part II."
18. Casagrande,A., "Seepage Through Dams" Contribution to Soil Mechanics, Boston Society of Civil Engineers, Boston,1937.
19. P.Novak,A.I.B.Moffat,C.Nalluri and R.Narayanan(20001),"Hydraulic Structures Third Edition," London and New York.
20. Duffy,M.,C.Hill, C.Whitaker, A. Chrzanowski, J. Lutes, and G. Bastin, 2001, "An automated and integrated monitoring program for Diamond Valley Lake in California", Preceedings of the 10th International symposium on Deformation Measurement.
21. Duscha and Jansen,1988, "Advanced Dam engineering for Design Construction , and Rehabilitation" New York.
22. USACE (1986), "Seepage Analysis and Control for Dams." Engineer manual, Washington, DC 20314-1000 ,United States.
23. http://www.geo-slope.com/products/seepw.aspx
24. Sam Johansson, February 1997, "Seepage Monitoring in Embankment Dams" Doctoral Thesis , Royal Institute of Technology, Stockholm, Sweden.
25. Bear, J. 1972. "Dynamics of fluid flow in porous media", Elsevier, New York